表3　生化学分析または遺伝子解析により確定診断された血管型 EDS 症例のまとめ

症例	家族	診断時年齢	性別	遺伝	初発症状(年齢、歳)	動脈系合併症				消化器系合併症	呼吸器系合併症	筋骨格系合併症	中枢神経合併症	遺伝子変異
						瘤(発症した動脈)	解離(発症した動脈)	破裂(発症した動脈)	頸動脈海綿静脈洞瘻					
1	1	25	男		[呼]喀血、気胸	+					喀血、気胸			ミスセンス
2	2	27	男		[動]下腿動脈瘤破裂	+		+						ミスセンス
3	3	20	男	孤発	[呼]喀血、肺出血						喀血、肺出血			ミスセンス
4	4	19	女	家族	[呼]気胸						気胸			スプライス
5	5	31	男		[消]S状結腸破裂					+(S状結腸破裂)				スプライス
6	6	32	男		[動]動脈瘤破裂	+		+						検出されず
7	7	42	女		[呼]気胸				+		気胸	内反足		スプライス
8	8	50	女	家族	[動]頸動脈海綿静脈洞瘻				+					ミスセンス
9	9	46	男		[消]腸間膜動脈閉塞、腸管壊死	+		+		+(腸間膜動脈閉塞、腸管壊死)				検出されず
10	10	17	男		[呼]血痰、気胸						血気胸、肺出血			ミスセンス
11	11	27	女	孤発	[消]結腸穿孔(17歳)		+(大腿)			+(結腸破裂)	血痰	靭帯損傷、脱臼(肩)	小脳低形成、梗塞	スプライス
12	12	23	女	家族	[皮]易出血、皮膚脆弱									ミスセンス
13		27	女	家族			+(椎骨)							ミスセンス
14	13	18	男	孤発	[呼]気胸						喀血、気胸	靭帯損傷		スプライス
15	14	23	男		[呼]血胸、気胸						血胸、気胸	内反足		ミスセンス
16	15	20	男	家族	[消]S状結腸破裂(19歳)					+(S状結腸破裂、空腸壊死)	気胸			スプライス
17		54	女	家族	家族検索							内反足、筋肉内出血		スプライス
18	16	28	男		[呼]血痰、気胸						血痰、気胸			スプライス
19	17	25	女		[筋]靭帯損傷							靭帯損傷		スプライス
20	18	14	男		[動]外腸骨動脈破裂			+(外腸骨)						スプライス
21	19	23	女		[皮]出血斑									スプライス
22	20	22	女	孤発	[消]直腸破裂					+(直腸破裂、S状結腸破裂)				スプライス
23	21	39	女		[動]動脈瘤解離	+	+							検出されず
24	22	30	男		[動]腎梗塞	+	+					靭帯損傷		ミスセンス
25	23	41	女		[動]解離性大動脈瘤	+	+							ミスセンス
26	24	19	男	家族	[呼]気胸(22歳)	+(冠)				+	気胸			ミスセンス
27		30	女	家族	[動]心筋梗塞(24歳)	+(冠)								ミスセンス
28	25	27	男	家族	[呼]気胸(25歳)			+(内腸骨)		+(S状結腸破裂)	気胸			ミスセンス
29		33	男	家族	家族検索	+(腎)	+(外腸骨)					靭帯損傷		ミスセンス
30	26	16	女	孤発	[呼]気胸(16歳)						血気胸、喀血			ミスセンス
31	27	26	女	孤発	[呼]血気胸(14歳)	+(内頸、椎骨、腎、内外腸骨)	+(外腸骨)		+	+(S状結腸破裂、小腸破裂)	血気胸、喀血	筋破裂	脳梗塞、脳出血	ミスセンス
32	28	20	女	孤発	[呼]気胸(20歳)	+(総肝)	+(内頸、外腸骨)		+		気胸、血気胸		梗塞	ミスセンス
33	29	43	男	家族	[呼]気胸(43歳)	+(冠)		+(腹腔)			血気胸、肺気腫	脱臼(股)		ミスセンス
34	30	28	女	家族	[動]頸動脈海綿静脈洞瘻(27歳)	+(内頸)	+(内頸、総腸骨)	+(脾)	+		気胸	内反足		スプライス
35	31	37	男	孤発	[呼]気胸(20歳)	+(脾)	+(腎)				気胸			スプライス
36	32	25	男	孤発	[動]後腹膜出血、腹腔内出血(25歳)	+(肝、胃)	+(外腸骨)	+(下腿)				内反足、靭帯損傷		スプライス
37	33	20	男	家族	[呼]気胸(18歳)		+(胸腔内)	+(腹腔内)			気胸			ミスセンス
38	34	38	男	孤発	[呼]気胸(17歳)			+(脱臼)			気胸			スプライス
39	35	37	男	家族	[動]脾動脈断裂(27歳)			+(脾)		+(食道穿孔、消化管出血)				ミスセンス
40		17	女	家族	卵巣出血(17歳)									ミスセンス
41	36	35	男	家族	[動]急性大動脈解離(21歳)	+(胸腹部)	+(胸腹部大、総頸、鎖骨下)			+(S状結腸破裂)	肺出血			ミスセンス

[呼]:呼吸器系合併症、[動]:動脈系合併症、[消]:消化器系合併症、[皮]皮膚合併症、[筋]:筋骨格系合併症

て現在、詳細な統一フォーマットを利用した患者データベースの構築を準備中である。これにより、詳細かつ漏れのない臨床情報の蓄積が期待できる。また、担当医と研究班が定期的に情報交換できるシステムを作ることにより、データベースをアップデートし続けることが可能となる。

本調査結果から合併症の概要が明らかになった。頻度は、動脈系63%、呼吸器系51%、筋骨格系29%、腸管24%、中枢神経系7％であった。臨床診断された7人を含む31人を調査したOderichらの報告では、動脈系24人（77%)、腸管破裂7人（23%)、気胸5人（16%)、関節脱臼5人（16%)、水晶体脱臼3人（10%）であった[6]。今回の調査では呼吸器系（気胸、血気胸、喀血または血痰、肺出血）の頻度が高かったといえる。また初発症状のなかでも最多であった（45%)。最近、本症における呼吸器系合併症の重要性が指摘されている。Kawabataらは、生化学分析または遺伝子解析により確定診断された血管型EDS患者9人の肺病変に関する詳細な病理学的検討結果を報告した。これによると、肺病変の根本は特発性の肺組織裂傷であり、これに基づき血腫や線維性結節が形成するとしている[7]。このことは喀血が多かった（17%）とする本調査結果と合致している。

36家系中33家系において*COL3A1*遺伝子変異が検出され、ミスセンス変異18家系（55%)、スプライス変異15家系（45%）であった。従来の報告に比べてスプライス変異の比率が高い傾向にあった。本調査のなかで、獨協医科大学皮膚科で解析された20家系では、ミスセンス変異45%、スプライス変異55%であり[8]、残る2施設で解析された13家系では、ミスセンス変異69%、スプライス変異31%であった。日本人患者ではスプライス変異が多い可能性[8]、または、患者収集上のバイアスである可能性が考えられた。変異が認められなかった家系においては、プロモーター領域の変異である可能性、他の遺伝子変異に基づき二次的にⅢ型コラーゲンの産生が低下している可能性が考えられる。さらに、遺伝子解析がmRNAを用いて行われているものであるため、nonsense-mediated decayを来す変異（ナンセンス変異、out-of-frameとなるスプライス変異や欠失など）を見逃している可能性がある。

以上、本邦初、世界でも大規模な部類に入る血管型EDS確定診断例の診療実態の概要を報告した。この結果は、新たに診断された患者、at riskの家族に対する遺伝カウンセリングにおいて、従来よりも詳細かつ的確な情報提供につなげられる点で有用と考えられる。今後、担当医と協力して本症患者の詳細かつ有用なデータベースを構築し、診療指針の確立を目指したい。

謝辞

遺伝子解析を担当したBanyar Tang Naing先生（日本医科大学医学部生化学・分子生物学)、秋元一三先生、牧野敦子先生、船越美由紀先生、生田目　貴先生（獨協医科大学総合医学研究所)、細胞培養を担当した河村理恵先生、田丸久美先生、涌井敬子先生（信州大学医学部遺伝医学・予防医学講座)、また研究全般においてご助言をいただきました島田隆先生（日本医科大学遺伝診療科、生化学・分子生物学）に深謝いたします。

本研究は、平成21～22年度厚生労働省難治性疾患克服研究事業「エーラスダンロス症候群（主に血管型および新型）の実態把握および診療指針の確立」の一環として行われた。

また、本研究は、第34回日本遺伝カウンセリング学会学術集会において、優秀演題賞を授与した。

文献

1）Beighton P, De Paepe A, Steinmann B, et al.: Ehlers-Danlos syndrome: Revised nosology, Villefranche, 1997. Am J Med Genet 77: 31-27, 1998.

2）Pepin MG, Byers PH(June 2006). Ehlers-Danlos syndrome, Vascular type. In: GeneReviews at Gene Tests: Medical Genetics Information Resource (database online). Copyright, University of Washington, Seattle, 1993-2006. Available at http://www.genetests.org. Accessed Aug 14, 2008.

3）渡邉淳，島田隆：血管型Ehlers-Danlos症候群の遺伝診療とその課題．遺伝診療をとりまく社会―その科学的・倫理的アプローチ，第1版，69-77，プレーン出版，東京，2007.

4）Pepin M, Schwarze U, Superti-Furga A, et al.: Clinical and genetic features of Ehlers-Danlos syndrome type IV, the vascular type. NEJM 342: 673-680, 2000.

5）Loeys BL, Schwarze U, Holm T, et al.: Aneurysm syndromes caused by mutations in the TGF-β receptor. NEJM 355: 788-798, 2006.

6）Oderich GS, Panneton JM, Bower TC, et al.: The spectrum, management and clinical outcomes of Ehlers-Danlos syndrome type IV: a 30-year experience. J Vasc Surg 42: 98-106, 2005.

7）Kawabata Y, Watanabe A, Yamaguchi S, et al.: Pleuropulmonary pathology of vascular Ehlers – Danlos syndrome: spontaneous laceration, haematoma and fibrous nodules. Histopathology 56: 944-950, 2010.

8）Shimokawa Y, Kosho T, Wataya-Kaneda M, et al.: Clinical and genetic features of 20 Japanese patients with vascular-type Ehlers-Danlos syndrome. Br J Dermatol 163: 704-710, 2010.

BJD
British Journal of Dermatology

Clinical and genetic features of 20 Japanese patients with vascular-type Ehlers–Danlos syndrome

Y. Shimaoka, T. Kosho,* M. Wataya-Kaneda,† M. Funakoshi,‡ T. Suzuki, S. Hayashi, Y. Mitsuhashi,§ T. Isei,¶ Y. Aoki,** K. Yamazaki,†† M. Ono,‡‡ K. Makino,§§ T. Tanaka,¶¶ E. Kunii*** and A. Hatamochi

Department of Dermatology, Dokkyo Medical University, School of Medicine, 880 Kitakobayashi, Mibu, Tochigi 321-0293, Japan
*Division of Clinical and Molecular Genetics, Shinsyu University Hospital, Matsumoto, Japan
†Department of Dermatology, Graduate School of Medicine, Osaka University, Osaka, Japan
‡Institute for Medical Science Dokkyo Medical University, Mibu, Tochigi, Japan
§Department of Dermatology, Tokyo Medical University, Tokyo, Japan
¶Department of Dermatology, Hirakata Hospital Kansai Medical University, Hirakata, Osaka, Japan
Departments of **Medical Genetics and ††Dermatology, Tohoku University School of Medicine, Sendai, Japan
‡‡Ono Dermatology Clinic, Toyota, Aichi, Japan
§§Department of Dermatology, Kumamoto University School of Medicine, Kumamoto, Japan
¶¶Department of Dermatology, Shiga Medical University, Ohtsu, Japan
***Department of Respiratory Disease, Gifu Prefectural Tajimi Hospital, Tajimi, Japan

Summary

Background Vascular-type Ehlers–Danlos syndrome (vEDS) is a severe autosomal dominant inherited disorder resulting from mutations within the α1 type III collagen gene (*COL3A1*). The majority of published mutations are base changes leading to the substitution of single glycine residues within the triple-helical domain of type III collagen. Although clinical characteristics and mutations in the *COL3A1* gene have been analysed for some patients from Europe and America, similar analyses have not yet been performed for Japanese patients with vEDS.

Objectives To analyse the genetic and phenotypic findings in Japanese patients with vEDS.

Methods We analysed the clinical features of 20 unrelated individuals with vEDS. To quantify type III collagen production, the fibroblasts were cultured with ^{3}H-proline, and the radiolabelled collagenous proteins were analysed using sodium dodecyl sulphate–polyacrylamide gel electrophoresis and fluorography. Mutations in *COL3A1* were detected by sequence analysis of cDNA from patients' fibroblasts and subsequently by a genomic DNA sequence analysis.

Results Thin and translucent skin with extensive bruising and hypermobility of the small joints were observed in about 90% of the patients, whereas the prevalence of serious clinical findings such as rupture/dissection/aneurysm of the arteries (30%) or rupture of the gastrointestinal tract (25%) was relatively low. Sequence analyses of the *COL3A1* gene demonstrated heterozygous point mutations leading to glycine substitution in only nine patients (45%), while heterozygous splice-site mutations at the junction of the triple-helical exons were observed in the remaining 11 patients (55%). The average type III collagen production level in the cultured dermal fibroblasts was 14·6% of the normal value. The types of complication were not associated with specific mutations in *COL3A1*.

Conclusion The analysis in the present series revealed a low frequency of patients presenting with serious clinical findings such as arterial rupture/arterial dissection/aneurysm and perforation or rupture of the gastrointestinal tract, and revealed a higher prevalence of splice-site mutations at the junction of the triple-helical exons than of glycine substitution mutations in *COL3A1*.

Correspondence
Atsushi Hatamochi.
E-mail: hatamo@dokkyomed.ac.jp

Accepted for publication
17 May 2010

Key words
clinical findings, COL3A1, Ehlers–Danlos syndrome (vascular type), mutations, type III collagen

Conflicts of interest
None declared.

DOI 10.1111/j.1365-2133.2010.09874.x

Ehlers–Danlos syndrome (EDS) is a heterogeneous group of heritable connective tissue disorders characterized by skin hyperextensibility, joint hypermobility, easy bruising and tissue fragility. According to the latest revised nosology, EDS can be classified into six major types: classical, hypermobility, vascular, kyphoscoliosis, arthrochalasia and dermatosparaxis.[1] Vascular-type EDS (vEDS; OMIM 130050) is an autosomal dominant inherited disorder with a frequency of 1 : 250 000;[2] vEDS is caused by a deficit in type III collagen resulting from heterogeneous mutations in the α1 type III collagen gene (*COL3A1*).[3] The remarkable reduction in type III collagen production arises from a dominant negative effect of the mutated collagen molecule in fibroblasts, crippling the function of normal collagen molecules produced by the wild-type allele. vEDS differs from other types of EDS in that it is associated with a higher risk of arterial rupture or aneurysm, gastrointestinal perforation or rupture, and uterine rupture during pregnancy, possibly leading to sudden death.[4] Establishing a correct diagnosis of vEDS is extremely important because the timing of the diagnosis can influence the patient's prognosis. Although some reports on the clinical characteristics and *COL3A1* mutations in patients with vEDS from Europe and America have been published,[5–9] similar analyses in Japanese patients with vEDS have not yet been done. Here, we describe the clinical characteristics, type III collagen production levels in cultured dermal fibroblasts, and *COL3A1* gene mutations observed in 20 Japanese patients with vEDS.

Materials and methods

Ethics

The study protocol was approved by the ethical committee of Dokkyo Medical University, School of Medicine (Japan). Informed consent was obtained after an explanation of the procedures to all the patients with vEDS and the control group volunteers.

Clinical data

The clinical data for the 20 unrelated individuals with vEDS are shown in Table 1.[10–14] To make a clinical diagnosis of vEDS we used the Villefranche nosology (1997).[1] The clinical diagnoses were confirmed by a biochemical demonstration of defective type III collagen production in cultured dermal fibroblasts and mutation analysis of *COL3A1*.

Cell culture

Skin biopsy specimens from all the patients with vEDS and 15 healthy subjects were obtained. Skin specimens from the healthy subjects were obtained from individuals undergoing plastic surgery after obtaining their informed consent. Dermal fibroblast cultures were established from the skin biopsy specimens using the outgrowth method, as described previously.[15] The cultures were maintained in Dulbecco's modified Eagle's medium (DMEM) containing 10% fetal bovine serum (FBS) in a CO_2 incubator at 37 °C.

Analysis of newly synthesized collagen

To confirm the reduction in type III collagen production in cultured dermal fibroblasts, collagen synthesis in cultured dermal fibroblasts was analysed as described previously.[16] Briefly, dermal fibroblasts were cultured to confluence in 100 × 20-mm dishes in DMEM containing 10% FBS. Then, the fibroblasts were incubated with DMEM containing 1% FBS and 5 μCi mL^{-1} of 2,3-[^{3}H]proline (Amersham Biosciences, Amersham, U.K.) in the presence of 50 μg mL^{-1} of L-ascorbic acid 2-phosphate for 24 h. Labelled proteins secreted into the culture medium were precipitated by the addition of 5% (final concentration) trichloroacetic acid, and the precipitate was dissolved in 0·05 mol L^{-1} acetic acid and digested with pepsin. Then, the labelled proteins were separated using sodium dodecyl sulphate–polyacrylamide gel electrophoresis (5% polyacrylamide gel containing 3·6 mol L^{-1} urea) in the presence or absence of 2-mercaptoethanol (which was added to reduce the samples). The radioactive bands were detected using fluorography. The level of type III collagen production in fibroblasts from each of the patients was determined as follows. First we performed densitometric scans of the bands of type III collagen and type I collagen [α1(I) + α2(I)] produced by the dermal fibroblasts obtained from the patients and from three age- and sex-matched controls. The densitometric scans were repeated three times. The level of type III collagen production was then normalized to the level of type I collagen production, and the type III collagen production levels of the patients were calculated as percentages of the levels of the controls, and they were expressed as mean ± SEM. The significance of the differences between the data from the controls and those from each patient was determined by Student's t-test.

Analysis of *COL3A1* sequence

First the cDNA and then the genomic DNA of each patient was analysed. Total RNA was extracted from cultured dermal fibroblasts using phenol/guanidinium isothiocyanate (Trizol reagent; Invitrogen, San Diego, CA, U.S.A.), and the cDNA was synthesized using the Rever-Tra Ace-α kit (Toyobo, Osaka, Japan). Polymerase chain reaction (PCR) was performed using primer pairs established to allow the analysis of the nucleotides encoding the entire triple-helical region from *COL3A1* cDNA. After confirming DNA amplification using agarose gel electrophoresis, we conducted direct sequencing using the ABI PRISM 3100 genetic analyser (ABI Advanced Biotechnologies, Columbia, MD, U.S.A.). Genomic DNA was extracted from the blood in accordance with a previously established method,[17] and the necessary portion was amplified using PCR and analysed by sequencing in a manner similar to that described above. The National Center for Biotechnology Infor-

Table 1 Summary of clinical findings, type III collagen production levels of fibroblasts and COL3A1 mutations in 20 Japanese patients with vascular-type Ehlers–Danlos syndrome

Case														Defects in COL3A1			
No.	Age (years)	Sex	Thin translucent skin	Extensive bruising	Characteristic facial appearance	Acrogeria	Hypermobility of small joints	Positive family history	Haemoptysis	Pneumothorax	Arterial aneurysm/ dissection/ rupture	Bowel rupture	Type III collagen production (%), mean ± SEM	Nucleotide change[a]	Protein effect[a]	Reference
1	23	F	+	+	+	–	+	+	–	–	–	–	10·7 ± 0·4	c.1151g>a	p.Gly384Asp (exon 18)	Present
2	30	M	–	+	+	–	+	+	–	–	+	–	29·2 ± 0·9	c.1330g>a[b]	p.Gly444Arg (exon 20)	8
3	17	M	–	+	–	?	+	–	+	+	–	+	12·3 ± 0·3	c.1511g>a	p.Gly504Asp (exon 21)	Present
4	50	F	+	–	+	?	–	+	–	–	–	–	11·7 ± 0·3	c. 1718g>a	p.Gly573Asp (exon 25)	Present
5	20	M	+	+	+	+	+	–	+	–	–	–	12·3 ± 0·6	c.1808g>a[b,c]	p.Gly603Asp (exon 26)	10
6	25	M	+	–	–	–	+	–	+	+	+	–	10·1 ± 0·2	c.1925g>a[b]	p.Gly642Asp (exon 29)	11
7	41	F	+	+	+	–	+	–	–	–	+	–	17·8 ± 0·3	c.2195g>a	p.Gly731Glu (exon 32)	Present
8	27	M	+	+	–	–	+	+	–	–	+	–	8·9 ± 0·4	c.2213g>a[b]	p.Gly738Val (exon 32)	8
9	23	M	+	+	+	+	+	+	+	+	–	–	11·3 ± 0·9	c.2528g>a[b]	p.Gly843Glu (exon 37)	12
10	25	F	+	+	+	–	+	–	–	–	–	–	14·6 ± 0·8	c.915_916ins GTAAGA	Insertion of 2 AA (VR)	Present
11	27	F	+	+	+	–	+	–	–	–	+	+	9·5 ± 0·2	g.IVS16+1G>A[b]	Exon (16) skipping	6
12	42	F	+	+	+	?	?	+	–	+	–	–	23·5 ± 0·8	g.IVS24+1G>A[b]	Exon (24) skipping	7,8
13	31	M	+	+	+	+	+	–	–	–	–	+	10·8 ± 0·3	g.IVS24+1G>A[b]	Exon (24) skipping	7,8
14	20	M	+	+	+	+	+	–	–	+	–	+	22·7 ± 0·2	g.IVS24+1G>A[b]	Exon (24) skipping	7,8,11
15	26	M	?	+	?	?	?	–	+	+	–	–	12·7 ± 0·3	g.IVS27+1G>C	Exon (27) skipping	Present
16	14	M	+	+	+	+	+	–	–	–	+	–	13·5 ± 0·7	c.2931_2931+ 15delGGTGAG TATAGTCAT	Exon (41) skipping	Present
17	22	F	+	–	–	+	+	–	–	–	–	+	20·2 ± 1·1	g.IVS41+2T>C[c]	Exon (41) skipping	Present
18	19	F	+	+	+	+	+	–	–	+	–	–	12·6 ± 0·6	g.IVS42+5G>A[b]	Insertion of 10 AA (VNSSTVSTSQ)	14
19	18	M	+	+	+	+	+	–	+	+	–	–	12·8 ± 0·2	g.IVS43+2T>C[b,c]	Exon (43) skipping	7
20	23	F	+	–	–	–	+	–	–	–	–	–	14·8 ± 0·6	g.IVS43+1G>a[b]	Exon (43) skipping	13

[a]Mutation numbering was performed based on the reference cDNA sequence (NM_000090), where +1 corresponds to the nucleotide A of ATG, the translation initiation codon. [b]Previously reported mutation. [c]De novo disease-causing mutation. AA, amino acid.

mation (NCBI) reference sequence, NM_000090, was used as the mRNA reference sequence and NCBI reference sequence, NG_007404.1, was used as the genomic DNA reference sequence.

Results

Clinical features of Japanese patients with vascular-type Ehlers–Danlos syndrome

Thin and translucent skin (Fig. 1a) was observed in 90% of the patients, and extensive bruising (Fig. 1b) was noted in 90%. The characteristic facial appearance (prominent eyes, thin nose and lobeless ears) (Fig. 1c) was present in 74% of the patients; acrogeria (Fig. 1d) was present in 50%, hypermobility of the small joints (Fig. 1e) was present in 94%, pneumothorax was present in 40%, a positive family history was present in 30%, arterial rupture/arterial dissection/aneurysm was present in 30% and perforation or rupture of the gastrointestinal tract was present in 25%. Of the 20 patients in this series, nine were women, but only one of them (case 12) had ever been pregnant, and none of them had ever experienced uterine rupture.

Analysis of type III collagen production by cultured fibroblasts

The amount of type III collagen produced in the medium was significantly reduced in all the cell cultures originating from patients with vEDS (Student's t-test, $P < 0{\cdot}01$ vs. age- and sex-matched controls) (Fig. 2). The average type III collagen production level in the cultured fibroblasts was 14·6% of the normal value.

Identification of the *COL3A1* mutation

In mutation analyses of the COL3A1 gene, heterozygous point mutations leading to a glycine substitution in the triple-helix region of *COL3A1* were demonstrated in only nine patients (45%) (Fig. 3a), while heterozygous splice-site mutations at the junction of the triple-helical exons, resulting in outcomes such as exon skipping, were observed in the remaining 11 individuals (55%) (Table 1). Of the 11 individuals, eight exhibited single base substitutions at the splice donor sites that resulted in the deletion of a single exon in the mRNA as the only splice alteration (Fig. 3b,c). Out of these eight patients, sequences encoded by exon 24 were deleted in three unrelated individuals, whereas deletions of exons 16, 27, 41, 43 and 45 were each identified in one individual. The remaining

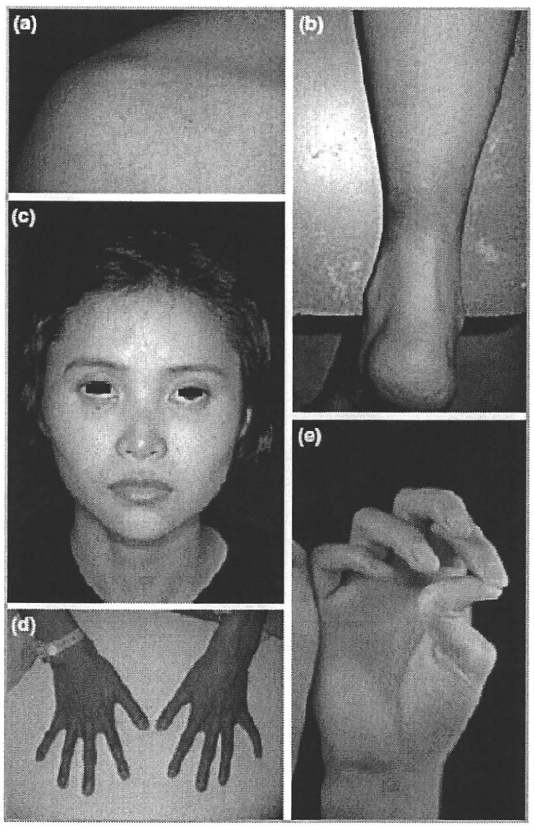

Fig 1. Clinical presentation of Japanese patients with vascular-type Ehlers–Danlos syndrome. (a) Thin, translucent skin (case 8); (b) extensive bruising (case 18); (c) characteristic facial appearance (case 10); (d) acrogeria (case 14); and (e) hypermobility of the small joints (case 20).

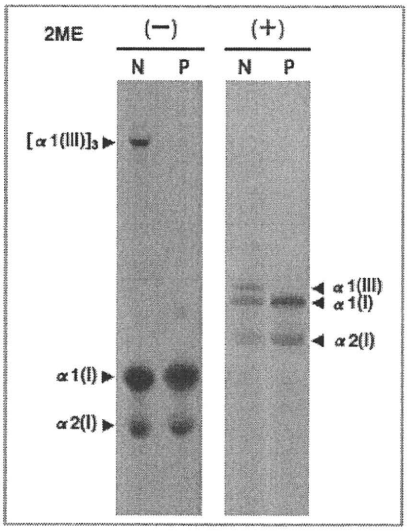

Fig 2. An example of the fluorograms for sodium dodecyl sulphate–polyacrylamide gel electrophoresis of collagen molecules obtained from the media of dermal fibroblast cultures of cells from a patient (P) (case 8) and an age- and sex-matched normal volunteer (N). 2ME, 2-mercaptoethanol.

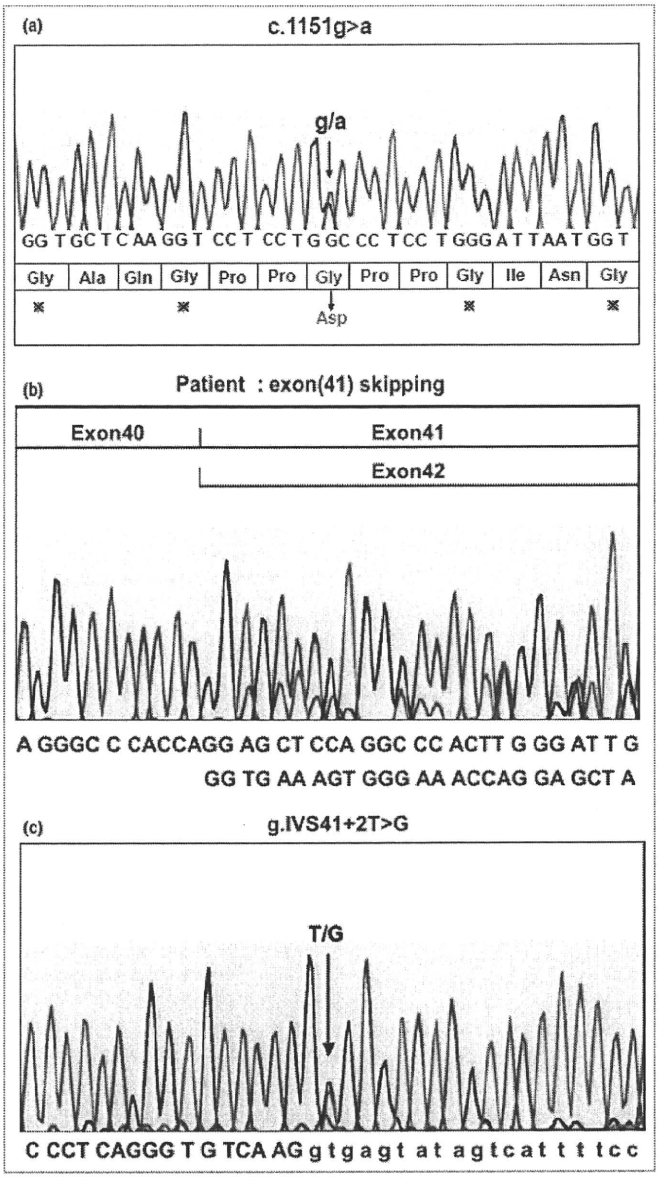

Fig 3. Sequence analyses of mutations of COL3A1. (a) An example of a heterozygous point mutation of COL3A1 that resulted in a glycine substitution. The arrow indicates the position of the point mutation. *Positions of glycine residues (case 1). (b, c) An example of a heterozygous point mutation of COL3A1 at splice donor sites that resulted in skipping of a single exon (case 17). (b) Analysis of COL3A1 cDNA from the patient's fibroblasts; one part of exon 42 was unreadable. (c) Analysis of the genomic DNA revealed a point mutation of T to G at donor splice site +2 of intron 42 (g.IVS41+2T>G). The arrow indicates the position of the point mutation.

three mutations were as follows: a small insertion at the end of the exon leading to the inclusion of partially inserted nucleotides in the mRNA (Fig. 4a) (case 10); a small deletion that removed the splice-junction sequences resulting in a single exon skipping (Fig. 4b) (case 16); and a point mutation at a donor site leading to a partial intron inclusion.[17] Of the 20 patients, six had a family history compatible with the disease (such as sudden death), and 14 were the first affected individuals in their families. In six of the 14, we were able to perform gene analyses in both parents (cases 5, 14, 16, 17, 18, 19) and were able to confirm de novo disease-causing mutations in four (cases 5, 16, 17, 19). The same mutation found in the patient was found in the mother of the patient in cases 14 and 18, but the mothers did not have any clinical manifestations of vEDS and they were diagnosed with vEDS genotypically.

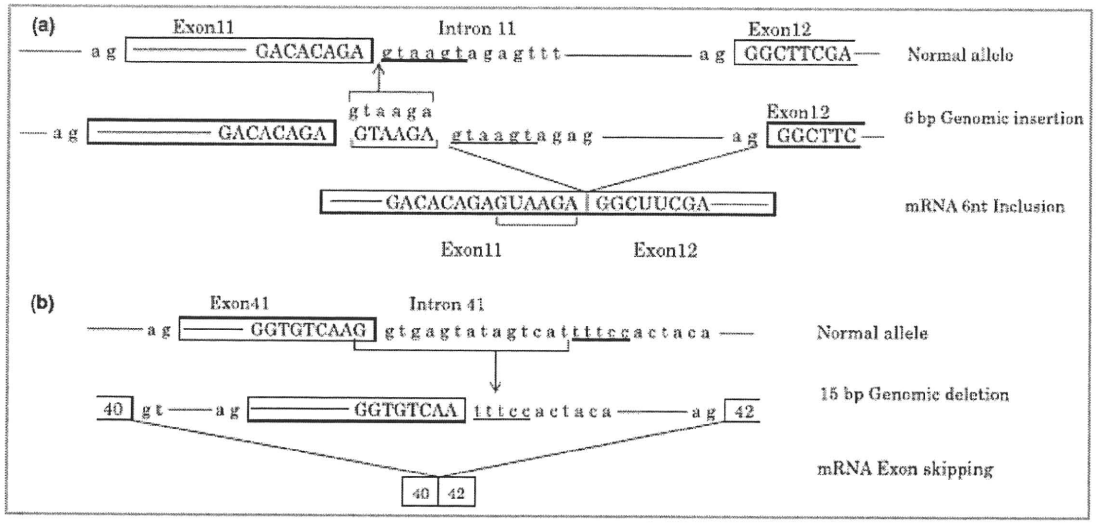

Fig 4. Schematic representation of two small genomic mutations of *COL3A1*. (a) A small insertion at the end of the exon, leading to the inclusion of partially inserted nucleotides in the mRNA (case 10). (b) A small deletion that removes the splice junction sequences, resulting in single exon skipping (case 16).

Discussion

vEDS is caused by abnormalities in the synthesis of type III collagen molecules that can be attributed to heterozygous mutations in *COL3A1*. Type III collagen is a structural protein that is widely distributed in the skin, blood vessels, ligaments and pleuroperitoneal linings.[5] The protein contains an uninterrupted central triple helix consisting of repeating cassettes of the general formula $(Gly\text{-}X\text{-}Y)_{343}$, in which the first residue is always glycine and where X and Y are frequently proline or lysine. To ensure the proper assembly of the α-monotrimers, the Gly-X-Y repeats must not contain skips, and the length of the triple helix must be the same for each α-chain. Three classes of *COL3A1* mutation have been described as molecular defects in individuals with vEDS.[5,7,8,18,19] Most mutations consist of substitutions of other amino acids for glycine in the Gly-X-Y repeats in the triple-helix region of *COL3A1*, and this class accounts for about two-thirds of all mutations reported.[5,8] A second class of mutations affects the splicing junctions of the triple-helix exons of *COL3A1*,[5,7,18] and this class accounts for about one-third of the mutations in previously reported cases. A third class of mutations[19] has been identified, i.e. mutations such as frameshift mutations that lead to premature termination codons that result in a nonfunctional *COL3A1* allele, but this class of mutations is very rare. Interestingly, in the present series, 55% of the *COL3A1* mutations in the Japanese patients with vEDS were splice-site mutations of the triple-helix exons, and the rest were glycine substitution mutations. Japanese individuals with vEDS might have a high incidence of splice-site mutations at the junction of the triple-helical exons in *COL3A1*.

Four novel mutations (in cases 1, 3, 4 and 7) in the present series were recognized as substitutions for glycine residues in the triple-helix region of *COL3A1*. There were also four novel mutations in the present series (in cases 10, 15, 16 and 17) that involved the splicing junctions of the triple-helix exons of *COL3A1*. The mutation IVS24+1G>A, which has been previously reported,[7,8] was found in three unrelated individuals with vEDS in the present series (cases 12, 13 and 14). Of these, two (cases 13 and 14) had frequent intestinal perforations, but the mother of one patient (case 14) who had the same mutation in *COL3A1* as her child did not have any serious complications. Case 12 also did not have any serious complications. These observations confirm the phenotypic heterogeneity of vEDS within the same family and among unrelated family members with the same *COL3A1* mutation.[8,20]

This report summarizes the symptoms of vEDS, the type III collagen production levels in cultured fibroblasts and the *COL3A1* mutations in 20 Japanese patients with vEDS. One other study has reported the symptoms of vEDS and the *COL3A1* mutations in five Japanese individuals with vEDS.[20] According to the latest revised nosology (Villefranche, 1997),[1] the major diagnostic criteria for vEDS include: (i) thin, translucent skin; (ii) arterial/intestinal/uterine fragility or rupture; (iii) extensive bruising; and (iv) a characteristic facial appearance. The presence of two or more of any of the major criteria is strongly suggestive of a diagnosis of vEDS, and laboratory testing is strongly recommended to confirm the diagnosis. In this report, the incidences of these major diagnostic findings, with the exception of arterial/intestinal/uterine fragility or rupture, were relatively high: 90% for thin, translucent skin; 90% for extensive bruising; and 68% for the characteristic facial appearance. A notable finding was the very high incidence of hypermobility of the small joints (94%), which is regarded as a minor criterion for vEDS. A

previous report[20] asserted that a high incidence of pneumothorax complications (80%) existed among their series of Japanese patients with vEDS; however, an incidence of only 40% for pneumothorax complications was observed in the present series. No associations between clinical findings and specific mutations were observed in the present series, similar to previous reports.[8,9]

The natural history of vEDS has been summarized according to the clinical complications, results of therapeutic intervention and information regarding survival.[8,9] Twenty-five per cent of the patients with vEDS had a first complication by the age of 20 years, and more than 80% had had at least one complication by the age of 40.[8] The analysis in the present series revealed a low frequency of cases presenting with serious clinical findings, such as rupture of the arteries or gastrointestinal tract. As these serious complications have been shown to increase with advancing age, the future development of serious complications among the patients in this series is extremely likely, as the mean age of the patients was relatively low (26 years) at the time of the analysis. Thus, measures for responding to emergencies and careful follow-up are needed for these patients.

What's already known about this topic?

- Although the clinical characteristics and mutations in the *COL3A1* gene have been analysed for some patients from Europe and America, similar analyses have not yet been performed for Japanese patients with vascular-type Ehlers–Danlos syndrome.

What does this study add?

- We describe the clinical characteristics, type III collagen production levels in cultured dermal fibroblasts and *COL3A1* gene mutations observed in 20 Japanese patients with vascular-type Ehlers–Danlos syndrome.
- The analysis in the present series revealed a higher prevalence of splice-site mutations at the junction of the triple-helical exons than of glycine substitution mutations in *COL3A1*.

Acknowledgment

We thank Miki Kanno and Takashi Namatame for their technical assistance.

References

1 Beighton P, De Paepe A, Steinmann B *et al.* Ehlers–Danlos syndrome: revised nosology, Villefranche. *J Med Genet* 1998; **77**:31–7.
2 Pepin MG, Byers PH. Ehlers–Danlos syndrome, vascular type. 2006. Available from: http://www.ncbi.nlm.nih.gov/bookshelf/br.fcgi?book=gene&part=eds4 (last accessed 27 May 2010).
3 Dalgleish R. The human collagen mutation database 1998. *Nucleic Acids Res* 1998; **26**:253–5.
4 De Paepe A, Malfait F. Bleeding and bruising in individuals with Ehlers–Danlos syndrome and other collagen vascular disorders. *Br J Haematol* 2004; **127**:491–500.
5 Pope FM, Narcisi P, Nicholis AC *et al.* *COL3A1* mutations cause variable clinical phenotypes including acrogeria and vascular rupture. *Br J Dermatol* 1996; **135**:163–81.
6 Kuivaniemi H, Kontusaari S, Tromp G *et al.* Identical G+1 to A mutations in three different introns of the type III procollagen gene (*COL3A1*) produce different patterns of RNA splicing in three variants of Ehlers–Danlos syndrome. IV. An explanation for exon skipping some mutations and not others. *J Biol Chem* 1990; **265**:12067–74.
7 Schwarze U, Goldstein JA, Byers PH. Splicing defects in the *COL3A1* gene: marked preference for 5′ (donor) splice-site mutations in patient with exon-skipping mutations and Ehlers–Danlos syndrome type IV. *Am J Hum Genet* 1997; **61**:1276–86.
8 Pepin M, Schwarze U, Superti-Furga A *et al.* Clinical and genetic features of Ehlers–Danlos syndrome type IV, the vascular type. *N Engl J Med* 2000; **342**:673–80.
9 Oderich GS, Panneton JM, Bower NM *et al.* The spectrum, management and clinical outcome of Ehlers–Danlos syndrome type IV: a 30-year experience. *J Vasc Surg* 2005; **42**:98–106.
10 Matsushita A, Takayanagi N, Ishiguro T *et al.* A case of Ehlers–Danlos syndrome suspected from pulmonary hematoma due to disruption of the lung. *Nihon Kokyuki Gakkai Zasshi* (Japanese edition) 2009; **47**:704–10.
11 Ishiguro T, Takayanagi N, Kawabata Y *et al.* Ehlers–Danlos syndrome with recurrent spontaneous pneumothoraces and cavitary lesion on chest X-ray as the initial complications. *Intern Med* 2009; **48**:717–22.
12 Sadakata R, Hatamochi A, Kodama K *et al.* A case of Ehlers–Danlos syndrome type IV, vascular type, demonstrated a newly recognized point mutation in the *COL3A1* gene. *Intern Med* 2010; in press.
13 Omori H, Hatamochi A, Koike M *et al.* Sigmoid colon perforation induced by the vascular type of Ehlers–Danlos syndrome: report of a case. *Surg Today* 2010; in press.
14 Okita H, Ikeda Y, Mitsuhashi Y *et al.* A novel point mutation at donor splice-site in intron 42 of type III collagen gene resulting in the inclusion of 30 nucleotides into the mature mRNA in a case of vascular type of Ehlers–Danlos syndrome. *Arch Dermatol Res* 2010; **302**:395–9.
15 Fleischmajer R, Perlish JS, Krieg T *et al.* Variability in collagen and fibronectin synthesis by scleroderma fibroblasts in primary culture. *J Invest Dermatol* 1981; **76**:400–3.
16 Hata R, Kurata S, Shinkai H. Existence of malfunctioning pro α2(I) collagen genes in a patient with a pro α2(I)-chain-defective variant of Ehlers–Danlos syndrome. *Eur J Biochem* 1988; **174**:231–7.
17 Hatamochi A, Ono M, Ueki H *et al.* Regulation of collagen gene expression by transformed human fibroblasts: decreased type I and type III collagen RNA transcription. *J Invest Dermatol* 1991; **96**:473–7.
18 Kuivaniemi H, Tromp G, Prockop DJ. Mutations in fibrillar collagens (types I, II, III, and XI), fibril-associated collagen (type IX), and network-forming collagen (type X) cause a spectrum of diseases of bone, cartilage, and blood vessels. *Hum Mutat* 1997; **9**:300–15.
19 Schwarze U, Schievink WI, Petty E *et al.* Haploinsufficiency for one *COL3A1* allele of type III procollagen results in a phenotype similar to the vascular form of Ehlers–Danlos syndrome, Ehlers–Danlos syndrome type IV. *Am J Hum Genet* 2001; **69**:989–1001.
20 Watanabe A, Kosho T, Wada T *et al.* Genetic aspects of vascular type of Ehlers–Danlos syndrome (vEDS, EDSIV) in Japan. *Circ J* 2007; **71**:261–5.

Biochemical and Biophysical Research Communications 405 (2011) 368–372

Contents lists available at ScienceDirect

Biochemical and Biophysical Research Communications

journal homepage: www.elsevier.com/locate/ybbrc

A novel mutation screening system for Ehlers-Danlos Syndrome, vascular type by high-resolution melting curve analysis in combination with small amplicon genotyping using genomic DNA

Banyar Than Naing [a], Atsushi Watanabe [a,b,*], Takashi Shimada [a,b]

[a] Department of Biochemistry and Molecular Biology, Nippon Medical School, Tokyo, Japan
[b] Division of Clinical Genetics, Nippon Medical School Hospital, Tokyo, Japan

ARTICLE INFO

Article history:
Received 29 December 2010
Available online 8 January 2011

Keywords:
Ehlers-Danlos syndrome, vascular type (vEDS)
COL3A1
Mutation screening
High-resolution melting curve analysis (hrMCA)

ABSTRACT

Ehlers-Danlos syndrome, vascular type (vEDS) (MIM #130050) is an autosomal dominant disorder caused by type III procollagen gene (*COL3A1*) mutations. Most *COL3A1* mutations are detected by using total RNA from patient-derived fibroblasts, which requires an invasive skin biopsy. High-resolution melting curve analysis (hrMCA) has recently been developed as a post-PCR mutation scanning method which enables simple, rapid, cost-effective, and highly sensitive mutation screening of large genes. We established a hrMCA method to screen for *COL3A1* mutations using genomic DNA. PCR primers pairs for *COL3A1* (52 amplicons) were designed to cover all coding regions of the 52 exons, including the splicing sites. We used 15 DNA samples (8 validation samples and 7 samples of clinically suspected vEDS patients) in this study. The eight known *COL3A1* mutations in validation samples were all successfully detected by the hrMCA. In addition, we identified five novel *COL3A1* mutations, including one deletion (c.2187delA) and one nonsense mutation (c.2992C>T) that could not be determined by the conventional total RNA method. Furthermore, we established a small amplicon genotyping (SAG) method for detecting three high frequency coding-region SNPs (rs1800255:G>A, rs1801184:T>C, and rs2271683:A>G) in *COL3A1* to differentiate mutations before sequencing. The use of hrMCA in combination with SAG from genomic DNA enables rapid detection of *COL3A1* mutations with high efficiency and specificity. A better understanding of the genotype–phenotype correlation in *COL3A1* using this method will lead to improve in diagnosis and treatment.

1. Introduction

Ehlers-Danlos syndrome, vascular type (vEDS), formerly called type IV EDS (MIM #130050) [1,2], is an autosomal dominant disorder caused by heterogeneous mutations of the gene encoding type III procollagen (*COL3A1*: MIM #120180) [3]. Its main clinical features are rupture of blood vessels or internal organs such as the uterus and bowel [4,5]. In the management of aneurysms, it is important to distinguish patients with vEDS due to a *COL3A1* mutation from other aneurysm syndromes with *FBN1* or *TGFBR* mutations, because tissue friability is different in these syndromes [6]. Since *COL3A1* is composed of 52 exons, most *COL3A1* mutations have been detected using a reverse transcriptase PCR (RT-PCR) direct-sequencing method with total RNA extracted from patient fibroblasts, which involves an invasive skin biopsy and cell culture [5]. Therefore, we considered an alternative rapid screening method to detect *COL3A1* mutations from genomic DNA.

Most mutation screening methods such as single-strand conformational polymorphism analysis [7], and denaturing high-performance liquid chromatography [8] require post-PCR manipulations, and are time consuming. A new mutation screening system termed "high-resolution melting curve analysis" (hrMCA) has recently been developed for rapid scanning of sequence variants [9–11]. The hrMCA is a closed-tube method that requires only one PCR reaction with fluorescence dye and melting analysis. Because of its ease of use, simplicity, flexibility, low cost, nondestructive nature, and high sensitivity (98%) and specificity (99.4%) [12], hrMCA is quickly becoming the tool of choice for mutation screening, especially of large genes [13].

In this study, we evaluated the hrMCA method using genomic DNA to screen the entire coding region of *COL3A1*. In addition, we applied detection of high frequency coding-region SNPs in

Abbreviations: vEDS, Ehlers-Danlos syndrome vascular type; *COL3A1*, type III procollagen gene; hrMCA, high-resolution melting curve analysis; SAG, small amplicon genotyping; cSNP, coding region single nucleotide polymorphism; Ct, cycle threshold; NMD, nonsense-mediated mRNA decay.

* Corresponding author at: Department of Biochemistry and Molecular Biology, Nippon Medical School, 1-1-5 Sendagi, Bunkyo-ku, Tokyo 113-8602, Japan. Fax: +81 3 5814 8156.
E-mail address: aw3703@nms.ac.jp (A. Watanabe).

0006-291X/$ - see front matter © 2011 Elsevier Inc. All rights reserved.
doi:10.1016/j.bbrc.2011.01.011

COL3A1 before sequencing, which are difficult to differentiate from mutations by hrMCA.

2. Materials and methods

2.1. Samples

We used 15 genomic DNA samples (8 validation samples with known *COL3A1* mutations to validate the hrMCA, and 7 clinically suspected Japanese vEDS patients) in this study. Informed consent was obtained from each patient. Genomic DNA samples were extracted from the peripheral blood using standard procedures. Clinically suspected vEDS patients were also analyzed by using the total RNA method (RT-PCR direct-sequencing) as described previously [5].

2.2. PCR for the hrMCA method

We designed 52 PCR primer pairs covering the entire coding region of *COL3A1*, containing 52 exons and the adjacent exon–intron junctions, by using the GenBank genetic sequence database (GenBank ID: NM_000090.3) as the reference (Supplementary Table 1). All primers were designed with the LightScanner Primer Design software program (Idaho Technology, UT, USA). The number of domains of each amplicon was predicted by Poland's algorithm (http://www.biophys.uni-duesseldorf.de/local/POLAND/poland.html) [14]. For each amplicon, the best annealing temperature for DNA amplification was determined by using a gradient temperature of 58 °C to 72 °C in a CFX96 Real-Time PCR detection system (Bio-Rad Laboratories, CA, USA) with control genomic DNA. DNA amplification was performed for each amplicon in 96-well microtiter plates with a 10-μl final volume containing 20 ng of genomic DNA, 200 μM each of deoxynucleotide triphosphates (dNTPs), 1× LCGreen Plus (Idaho Technology), 1× Ex Taq buffer, 0.5 U of Ex Taq enzyme (Takara Bio, Shiga, Japan), and 0.25 μM of each primer.

The thermocycling conditions were: 2 min at 95 °C, followed by 45 cycles of amplification consisting in 30 s at 94 °C and 30 s at gradient temperature from 62 °C to 67 °C. To promote heteroduplex formation, the samples were subsequently denatured by heating to 94 °C for 30 s and cooled to 25 °C for 30 s.

2.3. hrMCA

After the PCR, the plates were imaged in a 96-well LightScanner instrument (Idaho Technology) to examine the differences in the melting curves between the patient samples and the control. The plates were heated at 0.1 °C/s, and the fluorescence was measured from 70 °C to 98 °C. The melting curves were analyzed by using the LightScanner Call IT 1.5 software program (Idaho Technology) according to the manufacturer's protocol. All melting curves deviating from the wild-type curve and appearing as a different color in different plots potentially contain a variant.

2.4. Small amplicon genotyping (SAG) for coding-region SNPs (cSNPs) in COL3A1

We used a SAG method based on hrMCA to genotype three cSNPs with high frequency in *COL3A1* [15,16]. These include rs1800255:G>A, rs1801184:T>C, and rs2271683:A>G on exons 31, 33, and 49 of *COL3A1*, respectively. All three primer pairs were set on each exon so that the same primer pairs could be used for both genomic DNA and cDNA to detect the sequence discrepancies between genomic DNA and cDNA of the same patient (Supplementary Table 2).

DNA amplification was performed in a 96-well plate with a 10-μl final volume containing 4 μl of 2.5× high-sensitivity genotyping master mix (Idaho Technology), 1 μM of each primer, and 20 ng of genomic DNA or cDNA derived from 25 ng of total RNA. The thermocycling conditions were: 2 min at 95 °C, followed by 45 cycles of 30 s at 94 °C and 30 s at 72.6 °C (rs1801184 and rs2271683) or 74.7 °C (rs1800255). After PCR, the plate was imaged in a LightScanner and genotype identification was performed manually by using internal calibration.

2.5. Cycle sequencing

Samples from vEDS patients showing abnormal hrMCA profiles were sequenced with BigDye Terminator v3 (Applied Biosystems, CA, USA) according to the manufacturer's protocol and analyzed with ABI Prism 3130 (Applied Biosystems).

3. Results

3.1. Primer design and PCR optimization for hrMCA of COL3A1

The optimized PCR primers for the entire coding region of *COL3A1* are shown in Supplementary Table 1. The amplicon length was 124–330 bp, and the best annealing temperature was between 62 °C and 67 °C. There were 45 amplicons with two domains (which are a result of a high GC region with differences within the same amplicon) and seven amplicons with one domain. The expected number of domains by Poland's algorithm and the actual hrMCA-derived number of domains were almost the same (97% correct; data not shown). To maximize the sensitivity, the fragment of exon 49 was split into two amplicons.

3.2. COL3A1 mutation screening by hrMCA

After determining the best conditions, we set up a *COL3A1* mutation screening system based on hrMCA using genomic DNA. In this system, three patient samples and one control could be simultaneously analyzed in three 96-well plates (data not shown). When we started to check the differences in the melting curves between the patient samples and control by hrMCA, we obtained false positive different melting curves with the same nucleotide sequences in the same amplicon. These samples showed a large difference in Ct values, a fractional number of cycles in the PCR amplification curve of the real-time PCR, in the same amplicon detected by the real-time PCR detection instrument. The Ct value should be the same for each amplicon when the same primers are used to assay the mutant target [17]. In this study, the Ct value of each amplicon was 23–33 (mean = 25) (data not shown). Therefore, we used of all the samples with the same Ct value (Ct ± 0.7) within the same amplicon to reduce the false positives.

In eight validation samples, all mutations were correctly identified (Table 1A), including five missense (Fig. 1A–D) and three splice-site (Fig. 1H and I) mutations. Next, among clinically suspected vEDS patients, we found *COL3A1* mutations in seven patients, including five novel mutations, by the hrMCA method followed by sequencing (Table 1B). The mutations included two novel missense mutations (c.539G>A; Fig. 1E, and c.2150G>A; Fig. 1F), three splice-site mutations (one novel splice-mutation at c.897+1G>C; Fig. 1G and two at c.1662+1G>A; Fig. 1I), one novel nonsense mutation (c.2992C>T; Fig. 1J) and one novel deletion mutation (1-bp) in exon 32 (c.2187delA; Fig. 1K). We also evaluated six of the seven suspected clinical samples by the total RNA method, but the nonsense mutation found by the hrMCA in genomic DNA could not be detected by the total RNA method. The deletion mutation (c.2187delA) had a frameshift, leading to a

cSNPs is present in more than half of the European or Japanese population (http://www.ncbi.nlm.nih.gov/snp/). Therefore, to predict the common heterozygous cSNPs in *COL3A1* by the SAG method is important to reduce unnecessary sequencing. By the SAG method (Supplementary Table 2), both genomic DNA and cDNA from the same patient showed the same reproducible pattern for all three cSNPs (Fig. 2A–C), and we could clearly differentiate between the wild type (homozygous) and the SNP type (heterozygous) for all three cSNPs.

When this SAG method was applied for the patient with the nonsense mutation, the results showed different melting curves between genomic DNA and cDNA at two heterozygous cSNPs (rs1801184:T>C, and rs2271683:A>G) (Fig. 2D and E), suggesting that there were nucleotide discrepancies between genomic DNA and cDNA of the same patient. In this sample, we also found sequence discrepancies between genomic DNA and cDNA at the two heterozygous cSNPs and the nonsense mutation position (c.2992C>T) by sequencing (data not shown).

4. Discussion

We successfully established a method for mutation screening of the entire coding region of *COL3A1* for diagnosis of vEDS using gradient PCR reactions and the hrMCA method for genomic DNA, followed by sequencing of abnormal hrMCA exons. By this method, *COL3A1* mutations can be screened easily and rapidly with high sensitivity and specificity without an invasive skin biopsy procedure. In addition, this system enables to detect more *COL3A1* mutations caused by nonsense-mediated mRNA decay (NMD), nonsense mutations and small deletions that could not be detected by the conventional total RNA method.

For screening *COL3A1* mutations, two important factors were noted that indicate the superiority of the hrMCA method. First, *COL3A1* mutations are heterozygous in an autosomal dominant manner, which favors higher sensitivity and specificity in hrMCA than those for homozygous mutations [21,22]. The heterozygous detection rate has nearly 100% sensitivity [23], because heterozygotes form a proportion of heteroduplexes which melt differently to perfectly matched homoduplexes [24]. Second, the nucleotide levels in *COL3A1* mutations are preferable for hrMCA because a higher difference in the melting temperature results in a greater difference between the mutant melting curve and the control as determined by the hrMCA method [15]. The mutation patterns of G/A or T/C and G/T or A/C had a melting temperature that differed by 2 °C from the control, whereas the G/C or A/T patterns had only a 1 °C difference [12,15]. According to the reported *COL3A1* mutations, more than 85% of the missense and splice-site mutations showed G/A or G/T or T/C patterns (Human Gene Mutation Database (HGMD; http://www.hgmd.cf.ac.uk/ac/all.php)), which can be easily detected by the hrMCA method because of the greater melting temperature difference between the mutant and the wild type.

In determining the hrMCA conditions for the primer setting in each exon, the number of melting domains, which are a result of a high GC difference within the amplicon, should be considered. The number of domains for each amplicon could be predicted by Poland's algorithm before making the primers. Because hrMCA depends on the GC content of the amplicon, multiple domains can mask the presence of a mutation. Some researchers argue strongly for the use of small products, and against the use of multiple domains [25,26], but the optimal number of domains for hrMCA is still unclear [22]. In our experiment, we were able to generate the amplicon with shortest possible length in each exon containing one or two melting domains because the length of each exon of *COL3A1* is short.

It is important to reduce the false-positive results obtained by hrMCA. Samples with insufficient amplification should be reanalyzed from the PCR step in hrMCA [14]. However, it is sometimes difficult to determine whether amplification is sufficient. Therefore, we used the same Ct value (Ct ± 0.7) as a standard which is easy to evaluate, and the number of false-positive samples was reduced. For amplification of hrMCA samples, it is important to select the samples that have the same Ct value in each amplicon using a real-time PCR detection system.

In the present study, a nonsense mutation (c.2992C>T) could be detected only from genomic DNA by the hrMCA method, but not by the total RNA method. This discrepancy between genomic DNA and cDNA occurs because mRNA of the mutant allele does not mature as a result of NMD [27]. The deletion mutation (c.2187delA) in this study leads to a frameshift, causing a premature termination codon in exon 35 and is predicted not to be detected by the conventional total RNA method because of NMD [27,28]. In *COL3A1*, the reported mutations with NMD are very rare compared to other collagen gene mutations that cause diseases, because most *COL3A1* mutations have been detected previously using the total RNA method. The hrMCA method using genomic DNA in this study showed

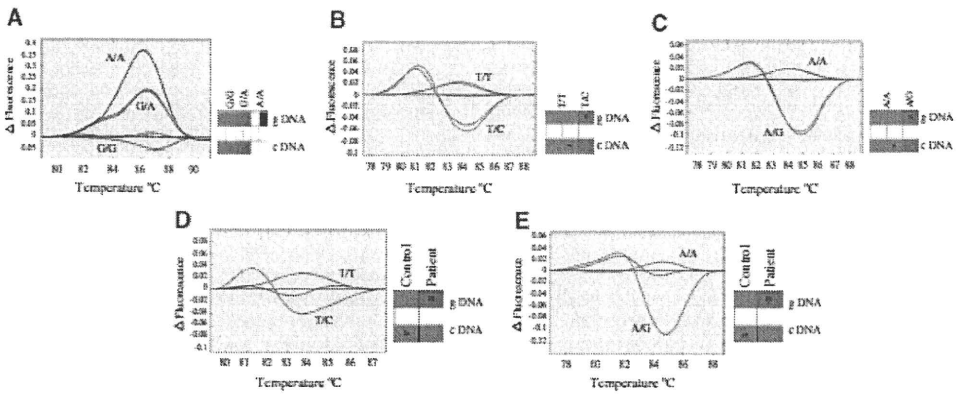

Fig. 2. *COL3A1* cSNP detection by the SAG method using genomic DNA and cDNA from the same individual: (A–C) Different melting curve patterns are shown between wild-type (homozygous) and SNP-type (hererozygous) in three common cSNPs. (A) rs1800255:G>A in exon 31 (G/G, G/A, A/A); (B) rs1801184:T>C in exon 33 (T/T, T/C); (C) rs2271683:A>G in exon 49 (A/A, A/G) genotypes. (D and E) Melting curve discrepancies between genomic DNA and cDNA are shown in *COL3A1* nonsense mutation patient compared to the control. (D) rs1801184:T>C in exon 33 and (E) rs2271683:A>G in exon 49.

higher mutation detection efficiency than the total RNA method. The number of mutations in *COL3A1*, including those caused by NMD, will likely be increased by mutation screening using genomic DNA. Screening of *COL3A1* mutations should be performed for the entire coding region of the gene by using genomic DNA for all patients showing the typical features of vEDS, regardless of whether there are negative findings based on a cDNA analysis, because nonsense mutations can occur at any position in the coding region.

Our SAG method enabled screening of the three most common cSNPs with high frequencies in *COL3A1*, and for prediction of cSNPs or mutations before sequencing. By the SAG method, nonsense mutations with any of the heterogeneous cSNPs of *COL3A1* can be predicted by checking for discrepancies between genomic DNA and cDNA. Therefore, our establishment of hrMCA for exon screening in combination with SAG of cSNPs from genomic DNA enables detection of *COL3A1* mutations with high sensitivity and specificity using a minimally-invasive procedure.

Emphasizing the importance of the new screening method, NMD has been shown to modulate the clinical outcome of genetic diseases [29]. In *COL3A1*, the phenotype severities might differ between different types of *COL3A1* mutations [28]. In the case of missense and splice-site mutations, production of the COL3A1 protein is reduced to one-eighth of the usual amount because of a dominant negative effect [2]. However, in the case of mutations with NMD, such as frame shift and nonsense mutations, the production of COL3A1 is reduced by half because of haploinsufficiency. Approaches to protect transcripts containing a premature termination codon from NMD could potentially be used as an alternative treatment [29]. A better understanding of the genotype–phenotype correlation in *COL3A1* using this method will lead to improve in the diagnosis and treatment of vEDS.

Acknowledgments

The authors wish to thank all of the patients and family members who participated in this study, and all the clinicians for referring the families. This work was supported in part by a grant from Grants-in Aid for Scientific Research (C) from the Ministry of Health, Education, Culture, Sports, Science and Technology of Japan, and by a Grant-in-Aid for Research on intractable disease from the Ministry of Health, Labor and Welfare of Japan.

Appendix A. Supplementary data

Supplementary data associated with this article can be found, in the online version, at doi:10.1016/j.bbrc.2011.01.011.

References

[1] D.P. Germain, Ehlers-Danlos syndrome type IV, Orphanet J. Rare Dis. 2 (2007) 32.
[2] A. Watanabe, T. Shimada, Vascular type of Ehlers-Danlos syndrome, J. Nippon Med. Sch. 75 (2008) 254–261.
[3] R. Dalgleish, The human collagen mutation database 1998, Nucl. Acids Res. 26 (1998) 253–255.
[4] M. Pepin, U. Schwarze, A. Superti-Furga, P.H. Byers, Clinical and genetic features of Ehlers-Danlos syndrome type IV, the vascular type, N. Engl. J. Med. 342 (2000) 673–680.
[5] A. Watanabe, T. Kosho, T. Wada, N. Sakai, M. Fujimoto, Y. Fukushima, T. Shimada, Genetic aspects of the vascular type of Ehlers-Danlos syndrome (vEDS, EDSIV) in Japan, Circ. J. 71 (2007) 261–265.
[6] B.L. Loeys, U. Schwarze, T. Holm, B.L. Callewaert, G.H. Thomas, H. Pannu, J.F. De Backer, G.L. Oswald, S. Symoens, S. Manouvrier, A.E. Roberts, F. Faravelli, M.A. Greco, R.E. Pyeritz, D.M. Milewicz, P.J. Coucke, D.E. Cameron, A.C. Braverman, P.H. Byers, A.M. De Paepe, H.C. Dietz, Aneurysm syndromes caused by mutations in the TGF-beta receptor, N. Engl. J. Med. 355 (2006) 788–798.
[7] M. Orita, H. Iwahana, H. Kanazawa, K. Hayashi, T. Sekiya, Detection of polymorphisms of human DNA by gel electrophoresis as single-strand conformation polymorphisms, Proc. Natl Acad. Sci. USA 86 (1989) 2766–2770.
[8] E. Holinski-Feder, Y. Muller-Koch, W. Friedl, G. Moeslein, G. Keller, J. Plaschke, W. Ballhausen, M. Gross, K. Baldwin-Jedele, M. Jungck, E. Mangold, H. Vogelsang, H.K. Schackert, P. Lohsea, J. Murken, T. Meitinger, DHPLC mutation analysis of the hereditary nonpolyposis colon cancer (HNPCC) genes hMLH1 and hMSH2, J. Biochem. Biophys. Methods 47 (2001) 21–32.
[9] C.T. Wittwer, G.H. Reed, C.N. Gundry, J.G. Vandersteen, R.J. Pryor, High-resolution genotyping by amplicon melting analysis using LCGreen, Clin. Chem. 49 (2003) 853–860.
[10] N. van der Stoep, C.D. van Paridon, T. Janssens, P. Krenkova, A. Stambergova, M. Macek, G. Matthijs, E. Bakker, Diagnostic guidelines for high-resolution melting curve (HRM) analysis: an interlaboratory validation of BRCA1 mutation scanning using the 96-well LightScanner, Hum. Mutat. 30 (2009) 899–909.
[11] E. Rouleau, C. Lefol, V. Bourdon, F. Coulet, T. Noguchi, F. Soubrier, I. Bieche, S. Olschwang, H. Sobol, R. Lidereau, Quantitative PCR high-resolution melting (qPCR-HRM) curve analysis, a new approach to simultaneously screen point mutations and large rearrangements: application to MLH1 germline mutations in Lynch syndrome, Hum. Mutat. 30 (2009) 867–875.
[12] G.H. Reed, C.T. Wittwer, Sensitivity and specificity of single-nucleotide polymorphism scanning by high-resolution melting analysis, Clin. Chem. 50 (2004) 1748–1754.
[13] R. Almomani, N. van der Stoep, E. Bakker, J.T. den Dunnen, M.H. Breuning, I.B. Ginjaar, Rapid and cost effective detection of small mutations in the DMD gene by high resolution melting curve analysis, Neuromuscul. Disord. 19 (2009) 383–390.
[14] H. Do, M. Krypuy, P.L. Mitchell, S.B. Fox, A. Dobrovic, High resolution melting analysis for rapid and sensitive EGFR and KRAS mutation detection in formalin fixed paraffin-embedded biopsies, BMC Cancer 8 (2008) 142.
[15] M. Liew, R. Pryor, R. Palais, C. Meadows, M. Erali, E. Lyon, C. Wittwer, Genotyping of single-nucleotide polymorphisms by high-resolution melting of small amplicons, Clin. Chem. 50 (2004) 1156–1164.
[16] J. Montgomery, C.T. Wittwer, R. Palais, L. Zhou, Simultaneous mutation scanning and genotyping by high-resolution DNA melting analysis, Nat. Protoc. 2 (2007) 59–66.
[17] J. Morlan, J. Baker, D. Sinicropi, Mutation detection by real-time PCR: a simple, robust and highly selective method, PLoS One 4 (2009) e4584.
[18] Y. Nishiyama, J. Nejima, A. Watanabe, E. Kotani, N. Sakai, A. Hatamochi, H. Shinkai, K. Kiuchi, K. Tamura, T. Shimada, T. Takano, Y. Katayama, Ehlers-Danlos syndrome type IV with a unique point mutation in COL3A1 and familial phenotype of myocardial infarction without organic coronary stenosis, J. Intern. Med. 249 (2001) 103–108.
[19] U. Schwarze, J.A. Goldstein, P.H. Byers, Splicing defects in the COL3A1 gene: marked preference for 5' (donor) spice-site mutations in patients with exon-skipping mutations and Ehlers-Danlos syndrome type IV, Am. J. Hum. Genet. 61 (1997) 1276–1286.
[20] O. Okamoto, T. Ando, A. Watanabe, F. Sato, H. Mimata, T. Shimada, S. Fujiwara, A novel point mutation in type III collagen gene resulting in exon 24 skipping in a case of vascular type Ehlers-Danlos syndrome, Arch. Dermatol. Res. 300 (2008) 525–529.
[21] R.H. Vossen, E. Aten, A. Roos, J.T. den Dunnen, High-resolution melting analysis (HRMA): more than just sequence variant screening, Hum. Mutat. 30 (2009) 860–866.
[22] C.T. Wittwer, High-resolution DNA melting analysis: advancements and limitations, Hum. Mutat. 30 (2009) 857–859.
[23] L.S. Chou, E. Lyon, C.T. Wittwer, A comparison of high-resolution melting analysis with denaturing high-performance liquid chromatography for mutation scanning cystic fibrosis transmembrane conductance regulator gene as a model, Am. J. Clin. Pathol. 124 (2005) 330–338.
[24] E.A. Takano, G. Mitchell, S.B. Fox, A. Dobrovic, Rapid detection of carriers with BRCA1 and BRCA2 mutations using high resolution melting analysis, BMC Cancer 8 (2008) 59.
[25] E.A. Tindall, D.C. Petersen, P. Woodbridge, K. Schipany, V.M. Hayes, Assessing high-resolution melt curve analysis for accurate detection of gene variants in complex DNA fragments, Hum. Mutat. 30 (2009) 876–883.
[26] M. Krypuy, A.A. Ahmed, D. Etemadmoghadam, S.J. Hyland, A. DeFazio, S.B. Fox, J.D. Brenton, D.D. Bowtell, A. Dobrovic, High resolution melting for mutation scanning of TP53 exons 5–8, BMC Cancer 7 (2007) 168.
[27] U. Schwarze, W.J. Schievink, E. Petty, M.R. Jaff, D. Babovic-Vuksanovic, K.J. Cherry, M. Pepin, P.H. Byers, Haploinsufficiency for one COL3A1 allele of type III procollagen results in a phenotype similar to the vascular form of Ehlers-Danlos syndrome, Ehlers-Danlos syndrome type IV, Am. J. Hum. Genet. 69 (2001) 989–1001.
[28] A. Plancke, M. Holder-Espinasse, V. Rigau, S. Manouvrier, M. Claustres, P. Khau Van Kien, Homozygosity for a null allele of COL3A1 results in recessive Ehlers-Danlos syndrome, Eur. J. Hum. Genet. 17 (2009) 1411–1416.
[29] M. Khajavi, K. Inoue, J.R. Lupski, Nonsense-mediated mRNA decay modulates clinical outcome of genetic disease, Eur. J. Hum. Genet. 14 (2006) 1074–1081.

RAPID PUBLICATION

AMERICAN JOURNAL OF medical genetics PART A

A New Ehlers–Danlos Syndrome With Craniofacial Characteristics, Multiple Congenital Contractures, Progressive Joint and Skin Laxity, and Multisystem Fragility-Related Manifestations

Tomoki Kosho,[1]* Noriko Miyake,[2] Atsushi Hatamochi,[3] Jun Takahashi,[4] Hiroyuki Kato,[4] Teruyoshi Miyahara,[5] Yasuhiko Igawa,[6] Hiroshi Yasui,[7] Tadao Ishida,[7] Kurahito Ono,[8] Takashi Kosuda,[9] Akihiko Inoue,[10] Mohei Kohyama,[11] Tadashi Hattori,[12] Hirofumi Ohashi,[13] Gen Nishimura,[14] Rie Kawamura,[1] Keiko Wakui,[1] Yoshimitsu Fukushima,[1] and Naomichi Matsumoto[2]

[1]Department of Medical Genetics, Shinshu University School of Medicine, Matsumoto, Japan

[2]Department of Human Genetics, Yokohama City University Graduate School of Medicine, Yokohama, Japan

[3]Department of Dermatology, Dokkyo Medical University, School of Medicine, Mibu, Japan

[4]Department of Orthopedics, Shinshu University School of Medicine, Matsumoto, Japan

[5]Department of Ophthalmology, Shinshu University School of Medicine, Matsumoto, Japan

[6]Department of Urology, Shinshu University School of Medicine, Matsumoto, Japan

[7]First Department of Internal Medicine, Sapporo Medical University, Sapporo, Japan

[8]Department of Orthopedics, Tomioka General Hospital, Tomioka, Japan

[9]Department of Pediatrics, Tomioka General Hospital, Tomioka, Japan

[10]Department of Surgery, Tomioka General Hospital, Tomioka, Japan

[11]Department of Surgery, JA Hiroshima General Hospital, Hiroshima, Japan

[12]Department of Orthopedics, Aichi Children's Health and Medical Center, Oobu, Japan

[13]Division of Medical Genetics, Saitama Children's Medical Center, Saitama, Japan

[14]Department of Radiology, Tokyo Metropolitan Kiyose Children's Hospital, Kiyose, Japan

Received 27 January 2010; Accepted 13 April 2010

We previously described two unrelated patients showing characteristic facial and skeletal features, overlapping with the kyphoscoliosis type Ehlers–Danlos syndrome (EDS) but without lysyl hydroxylase deficiency [Kosho et al. (2005) Am J Med Genet Part A 138A:282–287]. After observations of them over time and encounter with four additional unrelated patients, we have concluded that they represent a new clinically recognizable type of EDS with distinct craniofacial characteristics, multiple congenital contractures, progressive joint and skin laxity, and multisystem fragility-related manifestations. The patients exhibited strikingly similar features according to their age: *craniofacial*, large fontanelle, hypertelorism, short and downslanting palpebral fissures, blue sclerae, short nose with hypoplastic columella, low-set and rotated ears, high palate, long philtrum, thin vermilion of the upper lip, small mouth, and micro-retrognathia in infancy; slender and asymmetric face with protruding jaw from adolescence; *skeletal*, congenital contractures of fingers, wrists, and hips, and talipes equinovarus with anomalous insertions of flexor muscles; progressive joint laxity with recurrent dislocations; slender and/or cylindrical fingers and

Additional supporting information may be found in the online version of this article.
Grant sponsor: Research on Intractable Diseases, Ministry of Health, Welfare, and Labor, Japan; Grant Number: #2141039040; Grant sponsor: Shinshu Association for the Advancement of Medical Sciences; Grant sponsor: Grant-in-Aid for Exploratory Research of Young Scientists, Shinshu University.
*Correspondence to:
Tomoki Kosho, M.D., Department of Medical Genetics, Shinshu University School of Medicine, 3-1-1 Asahi, Matsumoto 390-8621, Japan.
E-mail: ktomoki@shinshu-u.ac.jp
Published online 14 May 2010 in Wiley InterScience
(www.interscience.wiley.com)
DOI 10.1002/ajmg.a.33498

progressive talipes valgus and cavum or planus, with diaphyseal narrowing of phalanges, metacarpals, and metatarsals; pectus deformities; scoliosis or kyphoscoliosis with decreased physiological curvatures of thoracic spines and tall vertebrae; *cutaneous*, progressive hyperextensibility, bruisability, and fragility with atrophic scars; fine palmar creases in childhood to acrogeria -like prominent wrinkles in adulthood, recurrent subcutaneous infections with fistula formation; *cardiovascular*, cardiac valve abnormalities, recurrent large subcutaneous hematomas from childhood; *gastrointestinal*, constipation, diverticula perforation; *respiratory*, (hemo)pneumothorax; and *ophthalmological*, strabismus, glaucoma, refractive errors. © 2010 Wiley-Liss, Inc.

Key words: a new type Ehlers–Danlos syndrome; craniofacial characteristics; multiple congenital contractures; joint laxity; talipes deformities; kyphoscoliosis; skin laxity; multisystem fragility; recurrent subcutaneous hematomas

How to Cite this Article:
Kosho T, Miyake N, Hatamochi A, Takahashi J, Kato H, Miyahara T, Igawa Y, Yasui H, Ishida T, Ono K, Kosuda T, Inoue A, Kohyama M, Hattori T, Ohashi H, Nishimura G, Kawamura R, Wakui K, Fukushima Y, Matsumoto N. 2010. A new Ehlers–Danlos syndrome with craniofacial characteristics, multiple congenital contractures, progressive joint and skin laxity, and multisystem fragility-related manifestations.
Am J Med Genet Part A 152A:1333–1346.

INTRODUCTION

The Ehlers–Danlos syndrome (EDS) is a heterogeneous group of heritable connective tissue disorders affecting as many as 1 in 5,000 individuals, characterized by joint and skin laxity, and tissue fragility [Steinmann et al., 2002]. The fundamental mechanisms of EDS are known to consist of dominant-negative effects or haploinsufficiency of mutant procollagen α-chains and deficiency of collagen-processing-enzymes [Mao and Bristow, 2001]. In a revised nosology, Beighton et al. [1998] classified EDS into six major types: (1) classical type (OMIM#130000) (causative gene, *COL5A1* or *COL5A2*; affected protein, α1(V) or α2(V) procollagen), (2) hypermobility type (OMIM#130020) (*TNXB*; tenascin-XB, in a small subset of cases), (3) vascular type (OMIM#130050) (*COL3A1*; α1(III) procollagen), (4) kyphoscoliosis type (OMIM#225400) (*PLOD*; lysyl hydroxylase), (5) arthrochalasia type (OMIM#130060) (*COL1A1* or *COL1A2*; α1(I) or α2(I) procollagen), and (6) dermatospraxis type (OMIM#225410) (*ADAMTS2*; procollagen I N-proteinase). Additional minor variants of EDS have been identified with molecular and biochemical abnormalities: Brittle cornea syndrome (OMIM#229200) (*ZNF469*) [Abu et al., 2008], EDS-like syndrome due to tenascin-XB deficiency (OMIM#606408) (*TNXB*; tenascin-XB) [Schalkwijk et al., 2001], progeroid form (OMIM#130070) (*β4GALT7*; xylosylprotein 4-beta-galactosyltransferase) [Kresse et al., 1987], cardiac valvular form (OMIM#225320) (*COL1A2*; α2(I) procollagen) [Schwarze et al., 2004], and EDS-like spondylocheirodysplasia (OMIM#612350) (*SLC39A13*; a membrane-bound zinc transporter) [Giunta et al., 2008].

We previously described two unrelated patients showing characteristic facial and skeletal features, with similarities to kyphoscoliosis type EDS but without lysyl hydroxylase deficiency [Kosho et al., 2005]. After observations of them over time and encounter with four additional unrelated patients including one reported by Yasui et al. [2003], we have concluded that they represent a new clinically recognizable type of EDS characterized by distinct craniofacial features, multiple congenital contractures, progressive joint and skin laxity, and progressive multisystem complications associated with tissue fragility including recurrent large subcutaneous hematomas. Here, we present detailed clinical courses of the six patients to delineate the disorder.

CLINICAL REPORTS

Patient 1

The patient is a now 16-year-old Japanese girl. Part of her history was described previously [Kosho et al., 2005]. She was the first child of a healthy mother and a healthy non-consanguineous father, both 19 years of age. She was born by normal vaginal delivery at 42 weeks of gestation. Her birth weight was 2,724 g (−1.3 SD), length 50.0 cm (−0.1 SD), and OFC 32.5 cm (−1.0 SD). She was admitted for the treatment of hypoglycemia, hyperbilirubinemia, and left talipes equinovarus (Fig. 1J). Her craniofacial features included a large fontanelle, hypertelorism, short and downslanting palpebral fissures, blue sclerae, a short nose with a hypoplastic columella, low-set and rotated ears, a high palate, a long philtrum, a thin upper lip vermilion, a small mouth, and micro-retrognathia (Fig. 1A). She had arachnodactyly, flexion-adduction contractures of bilateral thumbs, flexion contractures of the metacarpophalangeal (MP) and interphalangeal (IP) joints in the other fingers (Fig. 1E,F), and rigidity of bilateral hip joints. She suckled poorly, and was admitted again for the treatment of dehydration at age 1 month. Talipes equinovarus was treated with serial plaster casts, and was surgically corrected at age 2 years. Anomalous insertions of the flexor muscles were observed at the operation. Gross motor development was delayed: she sat at age 10 months and walked unassisted at age 2 years. Her skin was easily torn, but showed normal hemostasis in open wounds. Her face became longer with bushy and arched eyebrows and a pointed chin (Fig. 1B). At age 4 years, she developed a large subcutaneous hematoma over the occiput after falling, followed by acute hemorrhagic anemia that required admission and transfusion of hemostatic agents and packed red cells. During the admission, she was suspected to have EDS. At age 6 years, she developed a large subcutaneous hematoma over the temporo-occipital region after falling, requiring admission and intravenous administration of hemostatic agents. She had recurrent dislocations of the shoulders, elbows, and knees.

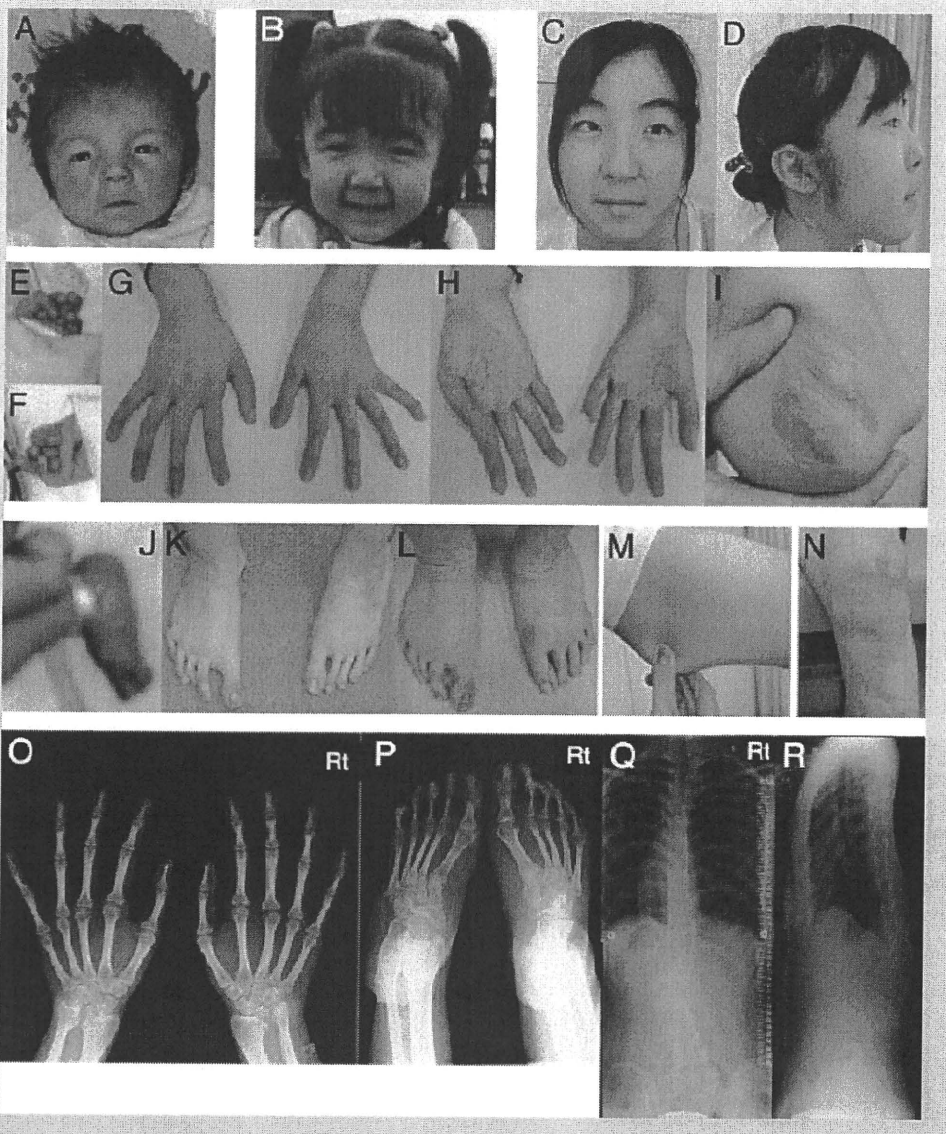

FIG. 1. Patient 1. Clinical photographs of the face at age 23 days (A), 3 years (B), and 16 years (C,D); the left (E) and the right (F) hands at age 23 days; the hands at age 16 years (G,H); the left elbow at age 16 years (I); the feet at birth (J), age 11 years (K), and 16 years (L); the skin on the left upper arm at age 16 years (M); and the left knee at age 16 years (N). Radiographs of the hands (O), the feet (P), and the spine (Q,R) at age 16 years. [Color figure can be viewed in the online issue, which is available at www.interscience.wiley.com.]

When first seen by us at age 7 years, she weighed 19.2 kg (−1.0 SD), height 123.8 cm (+0.8 SD), and OFC 51.5 cm (±0 SD). She had generalized joint laxity, a straight back with scoliosis, and cylindrical and slender fingers. Her skin was hyperextensible, bruisable, and fragile with multiple atrophic scars. Hyperalgesia to pressure such as measuring blood pressure at the upper arms was noted. Ophthalmological examinations showed microcornea and hyperopia. Otological examinations showed narrow middle ear spaces and hearing impairment of high-pitched sounds. Heart murmurs were not audible, and cardiac ultrasonography showed trivial mitral valve regurgitation. Her bladder was dilated with urinary retention and frequent cystitis, requiring manual pressure

voiding. She developed a large subcutaneous hematoma over the buttock after falling, requiring surgical drainage. Treatment with temporary intranasal administration of 1-desamino-8-D-arginine vasopressin (DDAVP) after injuries was started.

At age 11 years, she weighed 29.5 kg (−2 SD), height 148.1 cm (+0.2 SD), and OFC 54 cm (+0.2 SD). She had a slender face and a Marfanoid habitus with pectus excavatum and progressing talipes valgus and planus (Fig. 1K). Fine palmar creases and a ganglion on the left foot were noted. Hyperopia had improved and frequency of otitis media had decreased. Urinary retention persisted but manual pressure voiding was not necessary. Heart murmurs were audible, and cardiac ultrasonography showed moderate tricuspid valve regurgitation, prolapse of the tricuspid and mitral valves, and left-to-right shunt via a small atrial septal defect.

At age 12 years, menarche occurred. Kyphoscoliosis progressed with lumbago, necessitating a brace. The ganglion on the left foot was punctured and jellylike contents were suctioned, but soon it swelled again. Persistent urinary incontinence occurred, and urological examinations showed involuntary contractions and hypesthesia of the bladder with normal voiding function. She developed a large subcutaneous hematoma around the head and face after hitting the forehead on a door mirror, with a decline of hemoglobin concentration from 13.4 to 7.7 g/dl in several hours, and was admitted in an intensive care unit (ICU).

She had severe constipation (defecation once a week) and sometimes diarrhea (after having oily or watery foods), treated by medication of *Lactobaccilus* and lactulose from age 15 years. Large bowel sounds resembling a frog-croak were frequently heard. At age 16 years, acute gastric ulcer occurred in the antrum, leading to massive hematemesis. Gastric obstruction soon progressed, and treatment with a proton pump inhibitor and intravenous hyperalimentation (IVH) was not effective. A large thrombus developed at the site of inserting an IVH catheter, and an inferior vena cava filter was placed. Distal gastrectomy with Billroth I reconstruction was performed, complicated by a massive hematoma in the rectus sheath necessitating intranasal administration of DDAVP and transfusion of packed red cells and fresh frozen plasma. She attended a class for handicapped children from her junior high school days due to her physical fragility and mild learning disability.

When last seen by us at age 16 years, she weighed 49.4 kg (−0.4 SD), height 159.2 cm (+0.3 SD), and OFC 55.8 cm (+0.2 SD). Her face was slender with a protruding jaw (Fig. 1C,D). She suffered from lumbago because of progressive kyphoscoliosis. The distal IP joints in bilateral index to little fingers and the IP joints in bilateral thumbs could hardly be flexed or extended (Fig. 1G,H). The proximal IP joints in bilateral index to little fingers and the MP joints in all fingers could be flexed and extended, but could not be moved separately and smoothly (see supporting information Video 1 which may be found in the online version of this article). She had chronic dislocations of bilateral distal radio-ulnar joints and radial heads. Bilateral talipes valgus and planus progressed with extremely soft subcutaneous tissues at the heels (Fig. 1L), resulting in difficulty in walking. The IP joints in bilateral toes could not be moved and metatarsophalangeal joints could only be moved slightly. She had skin redundancy (Fig. 1M) and fragility with atrophic scars (Fig. 1N), fine palmar creases (Fig. 1H), and recurrent subcutaneous infections at the elbows (Fig. 1I) and the buttocks with fistula formation.

Patient 2

The patient is a now 32-year-old Japanese woman. Part of her history was described previously [Kosho et al., 2005]. She was born at term as the third child of a healthy 27-year-old mother and a healthy 37-year-old father, who were first cousins once removed. Her birth weight was 2,500 g (−2 SD) and two elder sisters were healthy. She suckled poorly, and was gavage fed for the first week of life. At age 9 weeks, she was admitted for the treatment of multiple contractures. Her craniofacial features included a large anterior fontanelle, hypertelorism, strabismus, short and downslanting palpebral fissures, a short nose with a hypoplastic columella, low-set and rotated ears, a long philtrum, a thin upper lip vermilion, a high palate, and micro-retrognathia (Fig. 2A). Skeletal features included extension contractures with ulnar deviation of bilateral wrists, flexion-adduction contractures of bilateral thumbs, flexion contractures of the MP joints in bilateral middle to little fingers, extension contractures of the distal IP joints in bilateral index to little fingers (Fig. 2E,F), bilateral talipes equinovarus (Fig. 2I), and a congenital dislocation of the right hip. Active movement of her fingers was poor. Mild skin hyperextensibility was noted. Talipes equinovarus and finger-wrist contractures were treated with serial plaster casts.

At age 1 year and 2 months, she underwent surgical corrections of bilateral talipes equinovarus. Anomalous insertions of the flexor muscles (the tibialis posterior to the talus [normal, navicular and cuneiform bones], the flexor digitorum longus to the abductor hallucis muscle [normal, bases of distal phalanges of four lesser toes], and the flexor hallucis longus to the calcaneus [normal, base of distal phalanx of hallux]) (Fig. 3) were shown to cause talipes equinovarus and inability to flex toes. Tendon sheaths of the muscles were hypoplastic, and surrounding tissues were fragile and hyperextensible. Skin hyperextensibility became more evident with frequent bruises. At age 2 years, dislocation of the right hip was treated through overhead traction and manual reduction under general anesthesia. Her tentative clinical diagnosis was Freeman–Sheldon syndrome.

Gross motor development was delayed: she raised her head at age 4 months, sat unassisted at 7 months, stood up assisted at 2 years and 6 months, cruised furniture at 3 years, and waked alone with short leg braces at 5 years. Generalized hypotonia and joint laxity became evident, and bilateral talipes valgus and cavus progressed (Fig. 2J). Her face became longer with drooping eyelids and bushy eyebrows (Fig. 2B). At age 6 years, dislocations of the left hip and the patella occurred, which were reduced manually. She also developed a subcutaneous hematoma around the left knee that required surgical drainage. She had constipation, and from incontinence and recurrent urinary tract infections associated with an atonic bladder and urinary retention. She had visual impairment from myopia and astigmatism, and impaired hearing for high-pitched sounds. At age 8 years, she developed a wound on the buttocks after falling, followed by bacterial infections and fistula formation, which lead to skin defects including decubitus necessitating plastic surgery. At age 11 years, she fell and developed a large subcutaneous hematoma over the head, requiring surgical drainage and transfusion of packed red cells. At age 12 years, she had dislocation of the left patella and left shoulder after minor injuries, which were

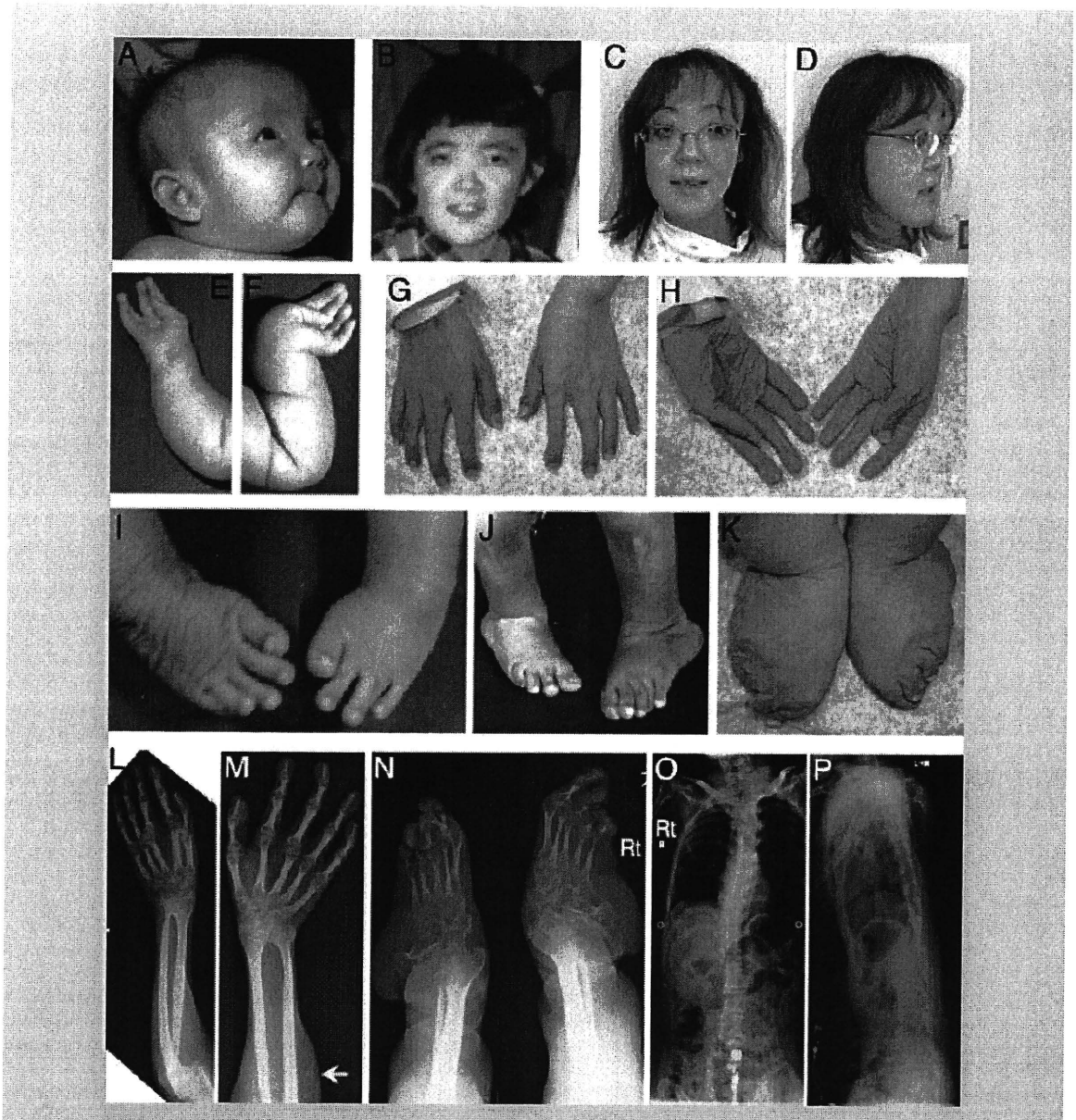

FIG. 2. Patient 2. Clinical photographs of the face at age 3 months (A), 8 years (B), and 28 years (C,D); the right arm at age 2 months (E); the left arm at age 3 months (F); the hands at age 28 years (G,H); and the feet at age 2 months (I), 6 years (J), and 28 years (K). Radiographs of the left (L) and the right (M) arms, the feet (N), and the spine (O,P) at age 28 years. An arrow indicates ectipic calcification (M). [Color figure can be viewed in the online issue, which is available at www.interscience.wiley.com.]

reduced manually. Her IQ was normal at 99. She attended a school for handicapped children because of limitations of daily activities bound to a wheelchair. Her clinical diagnosis was confirmed as EDS. At age 15 years, her height was 140 cm (−3.2 SD). She had marked muscle weakness with grip power 5 kg in the right and 2 kg in the left. She became exhausted easily. Frequent dislocations of the shoulders and elbows were reduced manually by her. Scoliosis was also noted.

At age 24 years, she underwent surgery for colonic perforation associated with diverticulitis. At the operation, multiple colonic

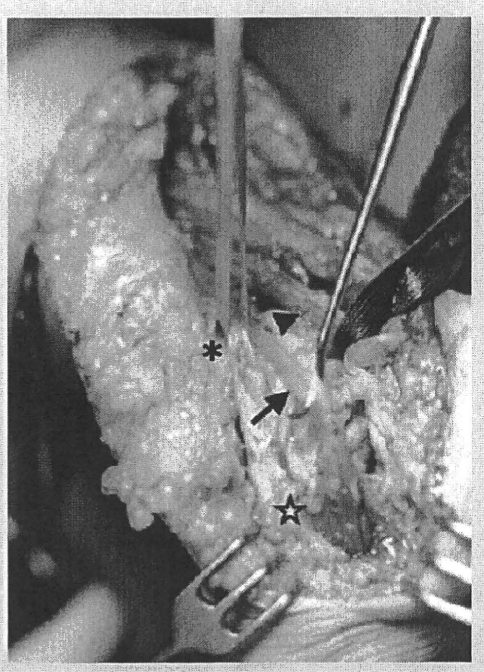

FIG. 3. An operative finding at postero-medial release in the right foot of Patient 2. Anomalous insertions of the flexor muscles are noted: the tibialis posterior muscle (*) to the talus, the flexor digitorum longus muscle (arrow) to the abductor hallucis muscle (blank star), and the flexor hallucis longus muscle (arrowhead) to the calcaneus.

diverticula were observed. At age 26 years, visual impairment progressed due to bilateral glaucoma with an elevation of intraocular pressure (IOP) to 20 mmHg in the right eye and 21 mmHg in the left eye, accompanied by a decreased visual field. At age 28 years, she suffered from a right pneumothorax, treated with chest tube drainage. Acute cystitis also occurred, and cystolithiasis was detected in the follow-up ultrasonography.

When seen by us at age 28 years, she was wheelchair-bound. She had a slender face with a protruding jaw (Fig. 2C,D). Her thorax was flat and thin. Her fingers were cylindrical. She had mild flexion contractures of the distal IP joints in bilateral index to little fingers, mild flexion-adduction contractures of bilateral thumbs (Fig. 2G,H), and chronic dislocations of bilateral distal radio-ulnar joints and the left radial head accompanied by ruptured tendon of the extensor pollicis longus muscle. She also had talipes valgus and cavus with extremely soft subcutaneous tissues at the heels (Fig. 2K). She could rarely flex or extend the left thumb or all toes. Her skin was redundant, bruisable, and fragile with atrophic scars. Prominent wrinkles in the palms showed acrogeria (Fig. 2H). She showed hyperalgesia to pressure such as measuring blood pressure at the upper arms. She had chronic subcutaneous abscesses with fistula formation at the elbows and buttocks. She suffered form severe constipation (defecation once a week) requiring oral laxatives and *Lactobaccilus*, but sometimes had diarrhea. Large bowel sounds resembling a frog-croak were frequently heard. Cardiac ultrasonography showed no structural or functional abnormalities in the mitral or aortic valve.

When last seen by us at age 31 years, she suffered from progressive visual field loss, although IOP was controlled within the range of 14–16 mmHg through topical administration of a prostaglandin F2 α derivative (latanoprost) and a β-adrenergic receptor blocker (timolol).

Patient 3

The patient, now a 32-year-old Japanese man, was the first child of a healthy 31-year-old mother and a healthy 25-year-old father, who were first cousins. His younger sister was healthy. He was delivered by vacuum extraction at 40 weeks of gestation. His birth weight was 3,300 g (+0.5 SD), length 52.0 cm (+1.3 SD), and OFC 35.0 cm (+0.8 SD). He was admitted for the treatment of orthopedic complications. He had a triangular face with a large skull, a large anterior fontanelle, hypertelorism, short and downslanting palpebral fissures, strabismus, a short nose with a hypoplastic columella, low-set and rotated ears, a long philtrum, a thin upper lip vermilion, a small mouth, and micro-retrognathia (Fig. 4A). His skeletal features included extension contractures of bilateral wrists, flexion-adduction contractures of bilateral thumbs, flexion contractures of the MP joints in bilateral index to little fingers, of the proximal IP joints in the right index and middle fingers, and of the distal IP joint in the left middle finger; extension contractures of the other IP joints (Fig. 4D,E), rigidity of bilateral hip joints, and bilateral talipes equinovarus (Fig. 4H). His skin was redundant with a lot of creases (Fig. 4D,E). Widely spaced nipples and bilateral cryptorchidism were noted. He was diagnosed as arthrogryposis. Talipes equinovarus was treated with serial plaster casts, and was surgically corrected at age 1 year and 8 months. He also underwent tendon transplantations for defects of tendons to bilateral thumbs, and orchiopexy.

At age 6 years, he developed a subcutaneous hematoma over the buttocks after falling, followed by bacterial infections and fistula formation. At age 8 years, a large subcutaneous hematoma occurred spontaneously over the head and progressed acutely with loss of consciousness, treated with emergency surgical drainage and transfusion of packed red cells. Large subcutaneous hematomas occurred in the left elbow at age 11 years, on the right shin followed by a rupture of another vessel, which spread the hematoma from the thigh to the ankle and made him bedridden for a month at age 14 years; on the right ankle necessitating admission at age 19 years, on the left arm making him bedridden for 2 months at age 26 and 27 years, and on the right shin making him bedridden for 2 months at age 29 years. He also suffered from recurrent joint dislocations of the right knee twice at age 9–10 years and the left shoulder five times at age 22–27 years. He was admitted for the treatment of bronchitis, leading to hearing impairment. At age 29 years, a rupture of a small intestine diverticulum was treated with emergency surgery.

When referred to us at age 30 years, his weight was 45 kg (−1.7 SD) and height 178 cm (+1.2 SD). He could walk independently but used a wheelchair when he went out. He had a skull with a

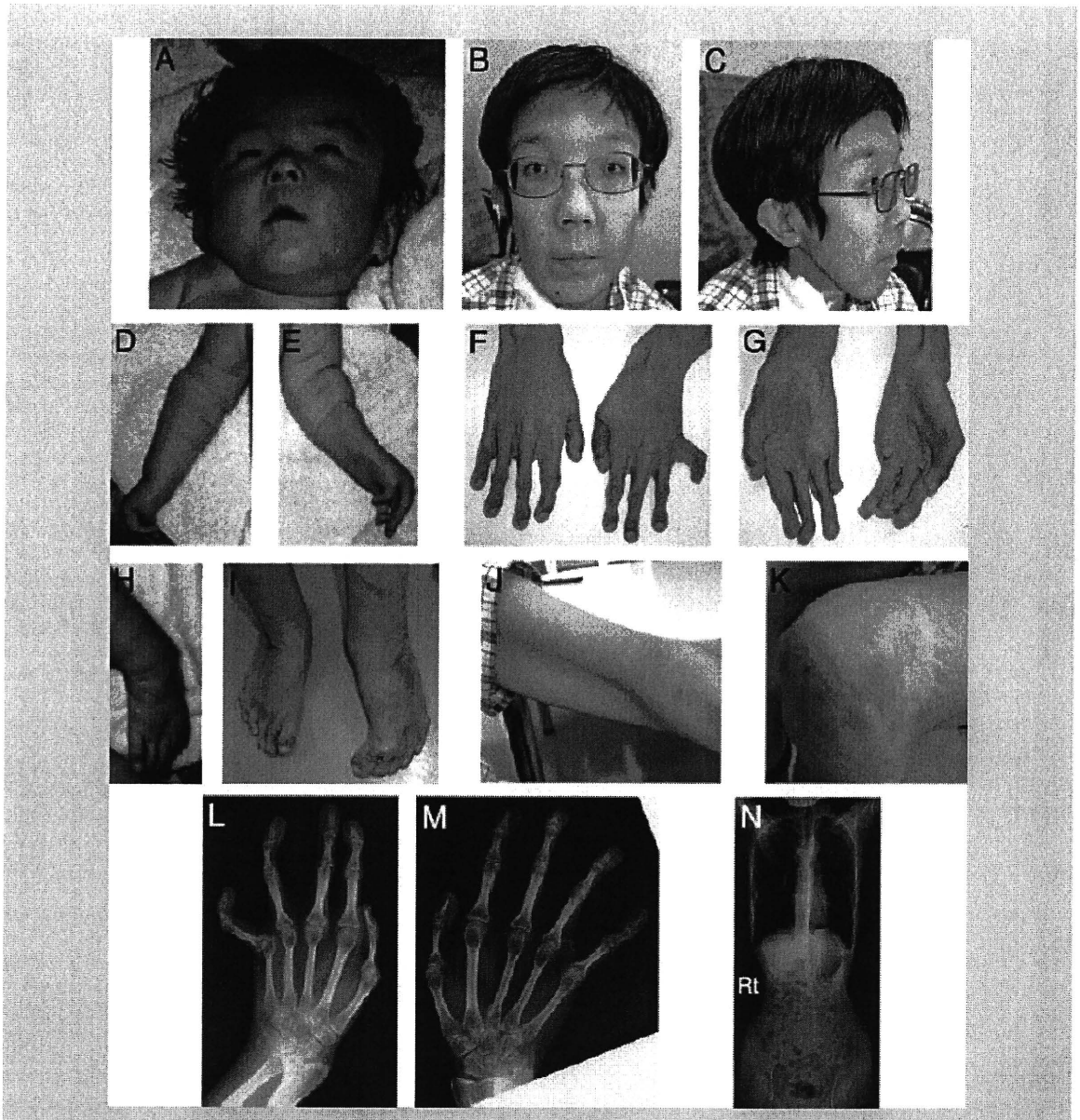

FIG. 4. Patient 3. Clinical photographs of the face in the neonatal period (A) and at age 30 years (B,C); the right (D) and the left (E) arms in the neonatal period; the hands at age 30 years (F,G); the left foot in the neonatal period (H); the feet at age 30 years (I); the skin on the left upper arm at age 30 years (J); and the left knee at age 30 years (K). Radiographs of the left (L) and the right (M) hands, and the spine (N) at age 31 years. [Color figure can be viewed in the online issue, which is available at www.interscience.wiley.com.]

prominent occiput and a lot of white hair, and a slender and asymmetric face with hypertelorism, strabismus, blue sclerae, a short nose with a hypoplastic columella, low-set rotated ears, a long philtrum, a thin upper lip vermilion, a high palate, crowded teeth, and a protruding jaw (Fig. 4B,C). He had a Marfanoid habitus with a flat and thin thorax and kyphoscoliosis. His fingers were slender and cylindrical. He had contractures of fingers and toes with limited flexion or extension (Fig. 4F,G,I), chronic dislocations of bilateral distal radio-ulnar joints and radial heads, and progressive talipes valgus and planus with extremely soft subcutaneous tissues at the